Ressortforschungsberichte zur kerntechnischen Sicherheit und zum Strahlenschutz

Quantitative Abschätzung des Strahlenrisikos unter Beachtung individueller Expositionsszenarien, Teil 2

only english report available

ProZES: a tool for assessment of assigned share of radiation in probability of cancer development (Part II)
- Vorhaben 3612S70030

Auftragnehmer:
Helmholtz Zentrum München - Deutsches Forschungszentrum für Gesundheit und Umwelt (GmbH)

A. Ulanowski
M. Eidemüller
D. Güthlin
J. C. Kaiser
E. Shemiakina
P. Jacob

Bundesamt für Strahlenschutz

Final report of the project StSch 3612S70030 "Quantitative Abschätzung des Strahlenrisikos unter Beachtung individueller Expositionsszenarien, Teil 2"

ProZES: a tool for assessment of assigned share of radiation in probability of cancer development (Part II)

Alexander Ulanowski   Markus Eidemüller   Denise Güthlin
Jan Christian Kaiser   Elena Shemiakina   Peter Jacob

ProZES

Helmholtz Zentrum München—German Research Center for Environmental Health,
Institute of Radiation Protection

Contents

Contents

List of Figures

List of Tables

Summary

Methodology and a corresponding computer program ProZES were developed to estimate the probability that a previous radiation exposure for a specific person and a given exposure situation has resulted in cancer (probability of causation or relationship between the exposure and the disease, Z). ProZES can provide the scientific basis to support making decisions on compensation claims due to cancer following occupational exposure to radiation. Starting from the results achieved in the first version of ProZES, when the general methodology and risk models for colon, stomach, lung, and female breast were implemented, the second stage of the ProZES development was focused on the development of risk models for all other cancer locations, including leukaemias and lymphomas as well as risk models for lung cancer after exposure to radon.

The models for estimating the cancer risks and the associated probability Z are mostly based on the observed cancer incidence in the cohort of the atomic bomb survivors in Hiroshima and Nagasaki. Most of the models are newly developed for the project. For the frequent types of cancer, specific models of radiation risk have been developed, while for the less common diseases the risk models were developed for the groups of functionally similar diseases. Since various models built upon the basis of the same data can result in different predictions for "dose-effect" relationships, so the method of "multi-model inference" is used for some types of cancer to derive risk factors, which are less dependent on individual models and take model uncertainties into account. Risk estimates for the Japanese population must be transferred to the German population. An essential element is the estimation of the uncertainty of the associated probability. ProZES was developed as a user-friendly stand-alone program, which can assess and present the individualised estimate of probability of relationship between radiation exposure and cancer graphically or in a textual form.

Zusammenfassung

Es wurden die Methoden und ein entsprechendes Computer-Programm ProZES entwickelt um die Wahrscheinlichkeit abzuschätzen, mit der eine vorangegangene Strahlenexposition bei einer bestimmten Person und bei einer gegebenen Expositionssituation zu einer Krebserkrankung geführt hat (Verursachungs- oder Zusammenhangswahrscheinlichkeit, Z). ProZES kann die wissenschaftliche Basis bereitstellen, um Entscheidungen zu Kompensationsklagen bei Auftreten von Krebs nach beruflicher Strahlenexposition zu unterstützen. Aufbauend auf der ersten Phase der Entwicklung von ProZES, die sich auf die Entwicklung von Risikomodellen für Krebs von Darm, Magen, Lunge und weibliche Brust konzentrierte, wurden in dieser zweiten Phase alle anderen Krebslokalitäten, einschließlich Leukämien und Lymphomen, berücksichtigt, sowie Modelle für Lungenkrebs nach Radon Exposition.

Die Modelle zur Abschätzung der Krebsrisiken und der Bestimmung der Zusammenhangswahrscheinlichkeit Z beruhen überwiegend auf den Inzidenzdaten für die Atombombenüberlebenden von Hiroshima und Nagasaki. Ein Großteil der Modelle wurde für das Projekt neu entwickelt. Spezifische Risikomodelle gibt es für die häufigsten Krebsarten, seltenere Krebsarten liegen als gruppierte Modelle vor. Da verschiedene Modelle eines Dosis-Wirkungs-Zusammenhangs auf Basis der gleichen Daten unterschiedliche Aussagen machen können, wird für manche Krebsarten die Methode der "Multi-Modell-Inferenz" benutzt, um Risikofaktoren abzuleiten, die weniger abhängig von einzelnen Modellen sind und Modellunsicherheiten berücksichtigen. Risikowerte von der japanischen Bevölkerung müssen auf die deutsche Bevölkerung übertragen werden. Ein wesentliches Element ist die Abschätzung der Unsicherheiten der Zusammenhangswahrscheinlichkeit. ProZES wurde als benutzerfreundliches Stand-Alone Programm entwickelt, das die individuelle Zusammenhangswahrscheinlichkeit graphisch oder textbasiert darstellen kann.

Preface

Ionising radiation is known to cause detrimental effects to human health, of which various malignancies and other late effects are among primary health concerns for people exposed to low doses of ionising radiation due to their professional activity or medical procedures. The established international system of radiological protection (ICRP, 2007) operates in a way to exclude the possibility of direct (deterministic) and to reduce, as much as practically affordable, the risk of late (stochastic) health effects for those occupationally exposed to radiation. This means, that for a person with occupational expose history being diagnosed with cancer, there are some chances that this newly diagnosed disease may be related to the preceding radiation exposure. Are these chances high or low? Is there a causal link between the disease and the exposure? Should this person be compensated for the health detriment or not? These are examples of questions, answers to which are needed for decision making in judicial considerations of compensation claims on diseases following professional exposure.

To help answering these questions, one wants to assess and to quantify radiation risk of the specific disease under individual-specific circumstances. To perform such assessment and quantification is the main goal to be achieved by using the software tool ProZES, which has been developed in Helmholtz Zentrum München in the period from 2009 to 2015 within frameworks of the research projects "Quantitative Abschätzung des Strahlenrisikos unter Beachtung Individueller Expositionsszenarien" StSch 3607S04570 (part 1) and StSch 3612S70030 (part 2) funded by the German Federal Ministry for the Environment, Nature Conservation, Building and Nuclear Safety (BMUB) and the German Federal Office for Radiation Protection (BfS).

The present report summarises outcomes of the second phase of the development in 2013–2015 and outlines the methodological basis and concepts underlying the tool. This report focuses on the scientific results obtained during implementation of the second part of the project; therefore, it complements results obtained at the previous stage (Jacob et al., 2013) as long as the latter are still valid or presents the new or modified material where the new results are different from the previous ones.

1 Introduction

Organisation of radiation protection at workplaces generally follows basic internationally adopted principles, which presume limiting radiation exposures to exclude (early) deterministic detrimental effects of radiation and to reduce as far as practically achievable probability of (late) harmful stochastic effects (ICRP, 2007). Malignant neoplasms of various kinds and, likely, circulatory diseases are currently accounted as main representatives of the stochastic effects of radiation exposure at low doses (UNSCEAR, 2011). The non-deterministic nature of these diseases means that appearance of harmful radiation effects is not pre-defined by the fact of exposure but can be characterised in terms of chances to get diseased, i.e. using probabilistic estimates.

Probabilistic link between radiation and harmful health effects means that people, whose occupational activity is related to additional radiation exposure, may have higher chances to get diseased. This fact justifies the idea of compensating health detriment due to occupation-related radiation exposure. However, the same diseases as those attributed to radiation may appear also among the general, non-exposed, population. Correspondingly, quantification of radiation-related and background risk appears as a decisive point for adjudication of compensation claims for malignancies appeared in those occupationally exposed to ionizing radiation in the past.

Principles and implementations of compensation systems vary among countries. A review and comparison of various national compensation systems can be found elsewhere (see e.g. Niu et al., 2010). In Germany, judicial decision on eligibility for compensation is based on an expert estimate of probability that the disease can be related to preceding radiation exposure. For quantification of the probability, the special tables (Chmelevsky et al., 1995) were in use. Since 2009, the new development, endorsed and supported by the German federal authorities, has been started to replace these tables by a tool capable of calculating radiation-attributed probability of a disease, accounting for the most recent epidemiological data and models and for their inherent uncertainties. The development resulted in appearance of ProZES (Jacob et al., 2013), which name abbreviates the German title of the tool: "Programm zur Berechnung der Zusammenhangswahrscheinlichkeit einer Erkrankung und einer Strahlenexposition", i.e. a program to calculate a probabilistic relationship between disease and radiation exposure. The first version of ProZES included radiation risk models for a number of the most frequent cancers of colon, stomach, female breast and lungs as well as established the main structure for calculations and uncertainty modelling. ProZES is in many aspects similar to its US-predecessor, program IREP (Kocher et al., 2008); however, the development of ProZES proceeded independently, following critical revisions of the existing models and techniques, fitting the new models, implementing novel principles, like multi-model inference (MMI). Special attention was given to careful consideration of inherent uncertainties. Discussions with the leading German and international experts in the field have also contributed significantly to the ProZES development.

Besides MMI, the following features were implemented in the first version of ProZES: stochastic

simulation of risk transfer from an epidemiological cohort to the target population, accounting for uncertainties specific to the risk estimates based upon epidemiological follow-up of the Life Span Study (LSS) cohort of the A-bomb survivors in Hiroshima and Nagasaki, original method of modelling uncertainties of radiation risk estimates at low doses, probabilistic modelling of minimal latency period. All models realised in the first version of ProZES are generally applicable to exposures due to low-LET radiation.

After successful completion of the first stage, a decision was made to continue the development in order to extend, based on already established computational framework, the list of accounted diseases and to include models for radiation risk due to high-LET exposure to radon and its radioactive progeny. The second stage of the development started in February 2013 and has been finished in October 2015. This report summarises results achieved after completion of the second stage and mostly presents detailed descriptions of the radiation risk models, originally developed on the basis of epidemiological incidence data of the LSS cohort during 1958–1998, made publicly available by Radiation Research Effects Foundation (Hiroshima, Japan).

This document does not include results obtained during the previous stage of the ProZES development in 2009–2012. Correspondingly, description of the risk models previously developed for explicit diagnoses (cancers of colon, stomach, lung, and female breast), details of implementation and of stochastic simulation techniques can be found in the first report on the ProZES development. That is, presented in the current report are the models and results, which are either completely new or significantly changed if compared to the previous report.

Changes also appeared on the technical side of ProZES. Originally developed as a mixed Fortran- and .NET-application, ProZES has been converted to and exists now as a pure .NET-based (i.e. based on Common Language Runtime, CLR) streamlined solution with improved compactness, reduced granularity (not using proprietary numeric libraries) and no loss of performance. This transition also creates preconditions for further modification of ProZES and converting it to a publicly available web-based application, like its US-counterparts IREP-NCI[1] and IREP-NIOSH[2].

The present report is complemented by four appendixes with supportive materials helpful to illustrate justification of the suggested solid cancers grouping (Appendix 1), comparison of the model baseline incidence rates for grouped solid cancers with data from population registries (Appendix 2), comparison of assigned share estimates calculated for some representative cases using the current versions of ProZES and IREP-NCI (Appendix 3), the ProZES help file with user's operational instructions (Appendix 4).

---

[1] https://www.irep.nci.nih.gov/irep/
[2] https://www.niosh-irep.com/irep_niosh/

2 Carcinogenic risk of radiation exposure

2.1 Probability of cancer causation

The probability that an individual gets a disease (cancer) is represented by the incidence rate of this disease in the population that matches the individual by gender, age, birth year and other relevant parameters. The disease incidence rate, λ, observed in such non-exposed population in the given calendar year is called 'baseline' incidence rate. Correspondingly, an effect of radiation exposure can be expressed as:

$$\lambda_r = \lambda + h, \tag{2.1}$$

where λ_r is the disease incidence rate in the target population following exposure (cancer cases per person-year, hereafter denoted as PY^{-1}); λ is the baseline incidence rate in the same non-exposed population (PY^{-1}); and h is the excess or deprivation incidence rate in the target population due to the exposure (PY^{-1}).

Generally speaking, the rate h can be positive or negative (the latter due to e.g. hormesis effect); however, because of incidence rate in population is non-negative by definition, $\lambda_r \geq 0$, so the excess rate h is bounded from below, i.e. $h \geq -\lambda$.

Following commonly adopted definitions, (see Land et al., 2003; BEIR, 2006; Niu et al., 2010) the fraction of the total incidence rate among the exposed population, which is due to rate h:

$$Z = \frac{h}{\lambda_r} = \frac{h}{\lambda + h} \tag{2.2}$$

is used in the present report to express a share of radiation-attributed rate in the total incidence rate, where Z is a notation of assigned share of radiation-related risk adopted in ProZES[1].

A graphic of Z as a function of excess rate h is shown in Fig. 2.1. As seen from the figure, negative values of the excess rate h translate to negative values of the assigned share: $Z \leq 0$. However, for compensation purposes, the only meaningful are positive excess rates in the area, indicated on the figure as "Detriment", where the radiation attributed share Z is bounded between 0 and 1, so it can be formally interpreted as probability that the disease is a radiation-attributed one and, consequently, Z can be alternatively called as 'probability of causation'.

The excess incidence rate h is also known as excess absolute risk (EAR):

$$h \equiv EAR, \tag{2.3}$$

while a ratio of the excess rate and the baseline rate is called excess relative risk (ERR):

$$\frac{h}{\lambda} \equiv ERR. \tag{2.4}$$

---

[1]From German word „Zusammenhangswahrscheinlichkeit": probability of link, probability of relation.
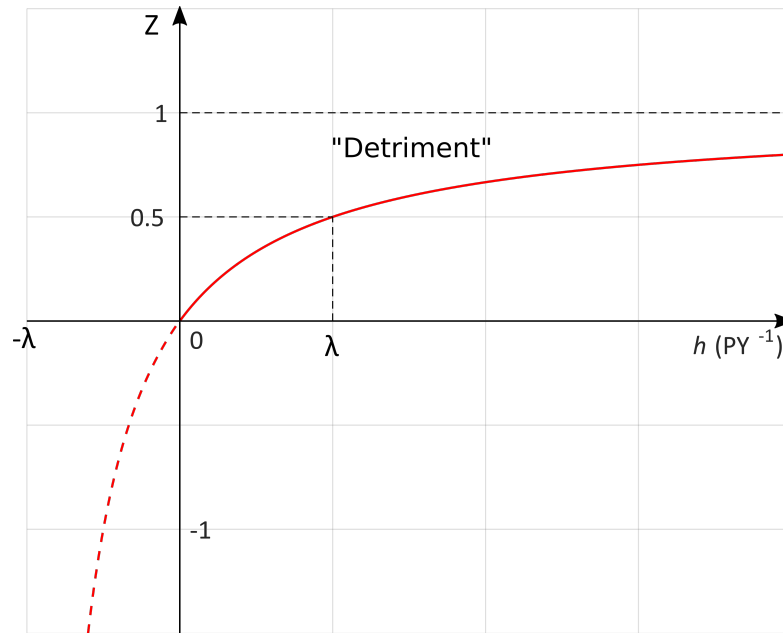
Figure 2.1: Share of radiation in the total incidence rate as function of excess rate

Using definitions (2.3) and (2.4), the assigned share (2.2) can be re-written in terms of excess absolute or relative risks:

$$Z = \frac{EAR}{\lambda + EAR} = \frac{ERR}{1 + ERR}. \tag{2.5}$$

2.2 Transport of risk between populations

Excess (h) and baseline (λ) rates in the equation (2.2) as well as EAR and ERR in the equation (2.5) are pertinent to the target population. These quantities are usually estimated from results of epidemiological studies of populations or groups exposed to radiation. Commonly, such epidemiological cohorts are formed from populations different to the target one due to a number of features, e.g. geographic, temporal, ethnic, gender, dietary, occupational and other ones. Correspondingly, risk estimates derived from epidemiological studies need to be adjusted or 'transported' to the target population. Hereafter, model estimates of rates or risk derived from epidemiological studies will be indicated by an index m in order to distinguish them from the similar quantities used for the target population.

Ideas for modelling of risk transfer from one population to another can be developed based on current notions of carcinogenic effects of radiation. Mechanistic description of carcinogenesis implies that development of a tumour is a complicated multi-stage process and radiation is thought to influence various stages of tumour development, so radiation effects can be roughly described as:

- additive, when radiation creates new centres of cancer development (affects 'starters'),

- multiplicative, when radiation accelerates development of existing modified or malignant cells (affects 'promoters').

Correspondingly, a transfer mode can be selected to be either additive, when excess absolute rate in the target population, h, is assumed to be the same as excess absolute rate in the studied cohort, h_m, or multiplicative, when the same is assumed for relative risks, h/λ and h_m/λ_m.

Technically, it means that the resulting excess rate for the target population can be modelled as a weighted sum of excess rates predicted by either transfer mode: additive or multiplicative. In this case, the excess rate in the target population is expressed as follows:

$$h = \underbrace{(1-f)\,h_m}_{\substack{\text{additive}\\\text{trasfer}}} + \underbrace{f\,\lambda\,\frac{h_m}{\lambda_m}}_{\substack{\text{multiplicative}\\\text{transfer}}}\,, \tag{2.6}$$

where f is the relative weight of the multiplicative transfer, $1-f$ is a complementary weight for the additive one, λ_m is the model baseline rate. Correspondingly, $f = 1$ results in pure multiplicative transfer, $f = 0$ in pure additive transfer, and other values in range $0 < f < 1$ are representative for mixed transfer mode. Denoting the ratio of the target population baseline and the model baseline as $B = \lambda/\lambda_m$, the equation (2.6) can be written as follows:

$$h = h_m\,(1 - f + f\,B)\,, \tag{2.7}$$

and, correspondingly, the probability of causation as:

$$Z = \frac{h_m\,(1 - f + f\,B)}{\lambda + h_m\,(1 - f + f\,B)}. \tag{2.8}$$

The baseline ratio B reflects differences existing between the target population and the model-based estimates pertinent to the epidemiological cohort. Besides obvious differences due to different geographical locations and customs of the populations, the difference also arises from the fact that model-based estimates and disease statistics for the target population are generally related to different time periods, so varying time trends in the disease incidence rates may additionally contribute significantly to value of the factor B.

Selection of the coefficient f which defines relative weights of either type of risk transfer is also not a straightforward task. Typically, it is unlikely that a decision on a type of the risk transfer for a specific cancer type can be judged based only on descriptive risk modelling, without using additional independent (e.g. biological) information. This means that if no preferred value or range of values can be advised for the factor f, then any value in the range from zero to one appear as equally probable. Under such circumstances, generation of the assigned share distribution can be realised by sampling a value of f from a uniform distribution: $f \sim U(0,1)$. This method of sampling the value of f is implemented in the current version of ProZES. Though, for simplified comparisons and for plotting, the best estimates of h and Z can be calculated using the mean value of the factor $\langle f \rangle = 0.5$.

2.3 Probability of causation after multiple exposures

Typically, consideration of compensation claims because of cancer following occupational exposure means necessity to consider probability of causation after a series of exposures occurred during the period of professional activity of a claimant. Taking into account that cancer incidence rates are small numbers (as a rule, not exceeding $10^{-2} PY^{-1}$ for the most frequently occurring cancers and the highest personal ages) and assuming that effects of different exposures on carcinogenesis are independent, then the cumulative effect of serial exposure can be represented as a sum of excess rates due to single exposures:

$$\lambda_r = \lambda + \sum_{i=1}^{n} h_i, \tag{2.9}$$

where h_i is the excess rates due to i^{th} exposure in a series of n exposures. Consequently, the probability of causation in the case of multiple exposures is

$$Z = \frac{\sum_i h_i}{\lambda + \sum_i h_i}, \tag{2.10}$$

and accounting for the mixed risk transfer (2.6) and assuming parameter f as fully correlated for the given individual at different exposure cases one finally gets for the probability of causation the following expression:

$$Z = \frac{(1-f)\sum_i h_{m,i} + f \sum_i h_{m,i} B_i}{\lambda + (1-f)\sum_i h_{m,i} + f \sum_i h_{m,i} B_i}, \tag{2.11}$$

where $h_{m,i}$ is the model excess rate after the ith exposure, $B_i = \lambda / \lambda_{m,i}$ is the baseline ratio and $\lambda_{m,i}$ is the model baseline rate for conditions specific to the ith exposure.

3 Thyroid cancer (ICD10:C73)

3.1 Model selection

The model for radiation-related risk of thyroid cancer has been selected after reviewing and evaluating the following models:

- the model of Jacob et al. (2006) based on analysis of thyroid cancer among children and adolescents in Ukraine and Belarus after the Chernobyl accident;

- the model of Preston et al. (2007) based on analysis of 40-year follow-up (1958–1998) in the LSS cohort;

- the model of Furukawa et al. (2013) based on an extended follow-up period (1958–2005) in the LSS cohort;

- the model of Jacob et al. (2014a) based on data for the LSS cohort for the follow-up period (1958–1998).

The study of Jacob et al. (2006) dealt with thyroid cancer incidence registered among children and adolescents (age at exposure less or equal to 18 years) in Belarus and Ukraine affected by exposure to radioiodine after the Chernobyl accident. Thyroid cancer incidence observed for these people in the period 1990–2001, i.e. up to 15 years since exposure, had been analysed and the radiation risk models were developed.

The other three studies (Preston et al., 2007; Furukawa et al., 2013; Jacob et al., 2014a) are based on an analysis of thyroid cancer incidence in the LSS cohort. These are not limited to children and young adults, so they were considered as preferred candidates for implementation in ProZES.

The model of Preston et al. (2007) has been based on incidence rate observed in the LSS cohort during 40-year follow-up, beginning from 1958, i.e. 13 years since exposure. This study included in the number of analysed cases those found due to autopsies conducted mainly before 1970 in a framework of a special program of autopsy studies for the LSS cohort members (Hayashi et al. 2010). That is, a number of occult[1] thyroid cancer cases had been added to the number of thyroid cancer cases analysed by Preston et al. (2007). Furukawa et al. (2013) re-analysed thyroid cancer risk in the LSS cohort for extended follow-up period up to 2005 and tried to eliminate a screening effect of the autopsy study by excluding cases of microcarcinoma (i.e. tumours with size less than 1 cm).

The analysis of thyroid cancer in the LSS cohort performed by Jacob et al. (2014a) has been conducted with publicly available incidence data for the LSS cohort in the period 1958–1998. In

---

[1]Cancer cases that otherwise would not become clinically relevant and diagnosed during the lifetime.
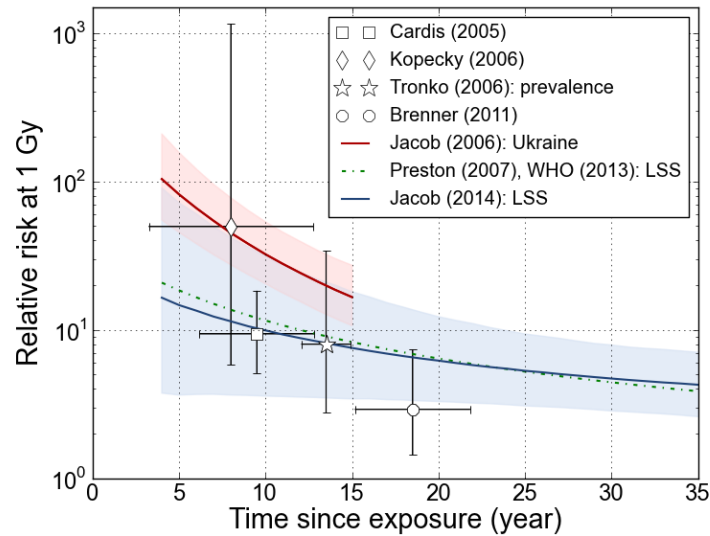
Figure 3.1: Relative risk of thyroid cancer as found in post-Chernobyl studies and computed with various models (age at exposure 7 years, gender-averaged)

this analysis, screening effect of medical surveillance for members of so-called Adult Health Study (AHS) has been explicitly modelled and found statistically significant. Moreover, the use of two different screening factors, reflecting different intensity of the autopsy studies before 1970 and after, was found significant and resulting in a better fit ($\Delta AIC = 12.32$) compared to the model of Preston et al. (2007) for the same data.

Despite of being based on the extended follow-up data, the model of Furukawa et al. (2013) has been rejected due to the following reasons: (a) effect of screening (parameter defined by AHS-membership) was independent on time; and (b) quadratic term in exponent function describing baseline incidence was insignificant and resulted in implausible extrapolations.

The above discussed models are compared to estimates derived in various post-Chernobyl studies (Cardis et al., 2005; Kopecky et al., 2006; Tronko et al., 2006; Brenner et al., 2011): relative risk in Fig. 3.1 and excess absolute risk in Fig. 3.2. The comparison is made for gender-averaged estimates and for cohort-averaged age at exposure 7 years, as typical to post-Chernobyl studies. The vertical error bars for experimental data and shaded areas for model estimates show their respective 95% confidence intervals. The horizontal error bars indicate time periods the experimental studies had been performed.

3.2 Description of the model selected for ProZES

In this subsection, the thyroid cancer risk model presented by Jacob et al. (2014a,b) is summarized. The model is based on data of cancer incidence observed in the LSS cohort in 1958–1998 as found in
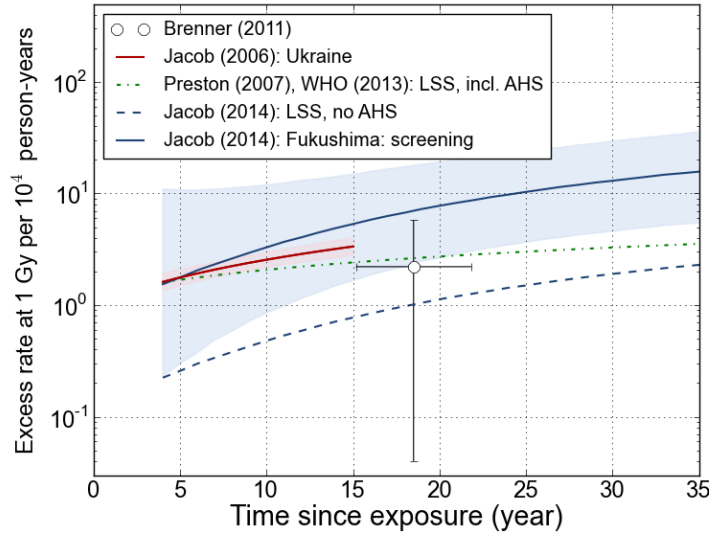
Figure 3.2: Excess absolute risk of thyroid cancer as found in post-Chernobyl studies and computed with various models (age at exposure 7 years, gender-averaged)

the file `lssinc07ahs.csv`, downloaded from the RERF website (http://www.rerf.or.jp). The dataset comprises 105,427 subjects and 471 cases of incidental thyroid cancer recorded in 2,764,725 person years (PYRs). The crude data is summarized in Preston et al. (2007, Table A18). The person-year weighted means are 23 years for age at exposure, 53 years for attained age, 60 years for age of cases and 105 mGy for the weighted dose to the thyroid. In the dose calculation, the neutron-related component was weighted with a relative biological effectiveness (RBE) of ten.

The baseline incidence rate $\lambda_0(s,a,e,c,AHS,NIC)$ depends on explanatory variables of sex s, attained age a, age at exposure e, city (Hiroshima: $c = 1$; Nagasaki $c = 2$), status of AHS participation (no: $AHS = 0$; yes: $AHS = 1$) and of having been in the city at the time of bombing (for distance from hypocenter <10 km: $NIC = 0$; otherwise: $NIC = 1$). The baseline incidence rate factorizes

$$\lambda_{0,LSS}(s,a,e,c,AHS,NIC) \times 10^4 = \lambda_{0,fit}(s,a,e) \, F_{scr}(a,e,AHS) \, g(c,NIC) \tag{3.1}$$

into a fit function common for all cohort members:

$$\lambda_{0,fit}(s,a,e) = \exp\left(\beta_{0,s} + \beta_{a_1,s}\ln\frac{a}{60} + \beta_{a_2,s}\ln^2\frac{a}{60} + \beta_{e_1,s}\frac{e-20}{10} + \beta_{e_2,s}\left(\frac{e-20}{60}\right)^2\right) \tag{3.2}$$

and an adjustment factor accounting for screening effect for the AHS members:

$$F_{scr}(a,e,AHS) = \exp\left(\beta_{AHS}(a-e)\,AHS\right), \tag{3.3}$$

where for non-zero factor AHS:

$$\beta_{AHS}(a-e) = \begin{cases} \beta_{AHS,1}, & a-e \geq 25 \text{ (AHS in 1970 and later);} \\ \beta_{AHS,1} + \beta_{AHS,2}, & a-e < 25 \text{ (AHS before 1970)} \end{cases} \tag{3.4}$$

Table 3.1: MLE estimates and confidence intervals (CIs) for the parameters of the ERR model for risk of thyroid cancer. CIs are calculated from the likelihood profile.

Parameter	Unit	MLE	Confidence interval for probability:	
			P = 0.68	P = 0.95
$\beta_{0,m}$	–	−0.39	(−0.62; −0.17)	–
$\beta_{0,f}$	–	0.53	(0.36; 0.70)	–
β_{city}	–	−0.22	(−0.33; −0.11)	–
β_{AHS}	–	0.21	(0.08; 0.33)	–
$\beta_{AHS,1970}$	–	0.33	(0.22; 0.44)	–
β_{NIC}	–	−0.47	(−0.61; −0.34)	–
$\beta_{a_1,m}$	–	1.9	(1.3; 2.5)	–
$\beta_{a_1,f}$	–	2.0	(1.5; 2.4)	–
$\beta_{a_2,f}$	–	−0.75	(−1.30; −0.24)	–
$\beta_{e_1,m}$	yr^{-1}	0.091	(n.a.; 0.19)	–
$\beta_{e_1,f}$	yr^{-1}	−0.24	(−0.33; −0.16)	–
$\beta_{e_2,f}$	yr^{-1}	0.080	(0.060; 0.098)	–
α_d	Gy^{-1}	1.07	(0.71; 1.51)	(0.44; 2.04)
α_e	–	−0.59	(−0.89; −0.32)	(−1.20;−0.08)
α_a	yr^{-1}	−1.03	(−1.89; −0.16)	(−2.74; 0.70)
α_s	–	0.11	(−0.16; 0.42)	(−0.52; 0.77)

and a factor accounting for residential status (city and 'not-in-the-city' factor — NIC):

$$g(c, NIC) = \exp\left(\beta_c (c - 1) + \beta_{NIC} NIC\right). \tag{3.5}$$

The baseline model of Preston et al. (2007) is nested to the baseline model of the present analysis. In the further calculations, city- and NIC-status have been averaged out with weights defined from the number of cancer cases observed in each of the sub-groups of the LSS cohort. For the dose response an ERR model was chosen using the form

$$ERR(s, e, a) = \alpha_d D \exp\left[\alpha_s s + \alpha_a \ln \frac{a}{60} + \alpha_e \frac{e - 20}{10}\right], \tag{3.6}$$

where α are the model parameters, D is the weighted thyroid dose and the parameter s equals to $+1$ for females and to $−1$ for males.

The original ERR model of Preston et al. (2007) used 22 parameters with a deviance of 3037.97 (Akaike Information Criterion, AIC=3081.97). The present model consumed 17 parameters and yielded a deviance of 3037.65 (AIC=3069.65). Maximum likelihood estimates (MLE) and confidence intervals are given in Table 3.1. Estimates of the ERR at 1 Gy from Preston et al. (2007) and the present study differ by less than ten percent. The confidence intervals are quite symmetrical.
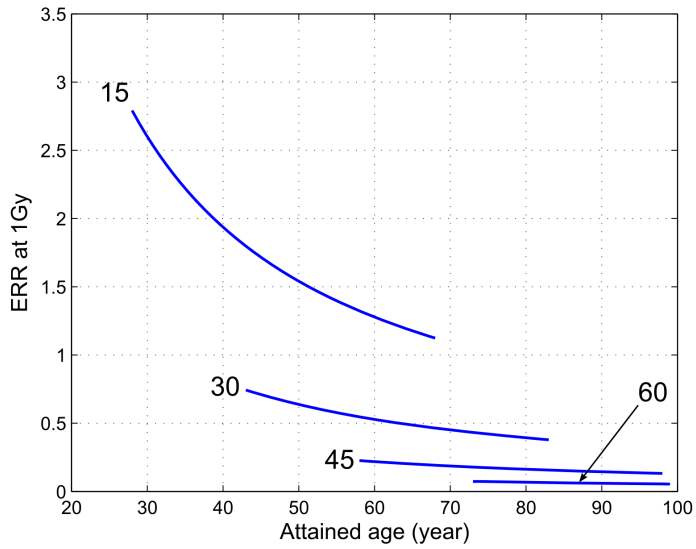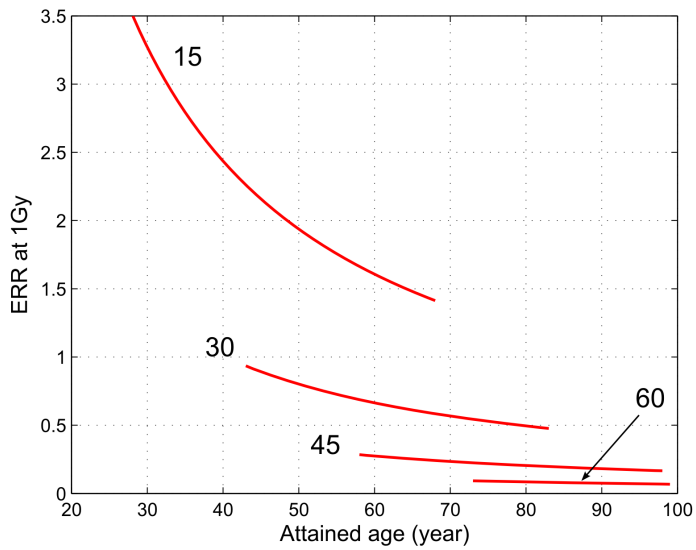
(a) male

(b) female

Figure 3.3: Excess relative risk of thyroid cancer after exposure at various ages (shown by numbers) to dose 1 Gy for males (a) and females (b) as estimated using the model of Jacob et al. (2014a)
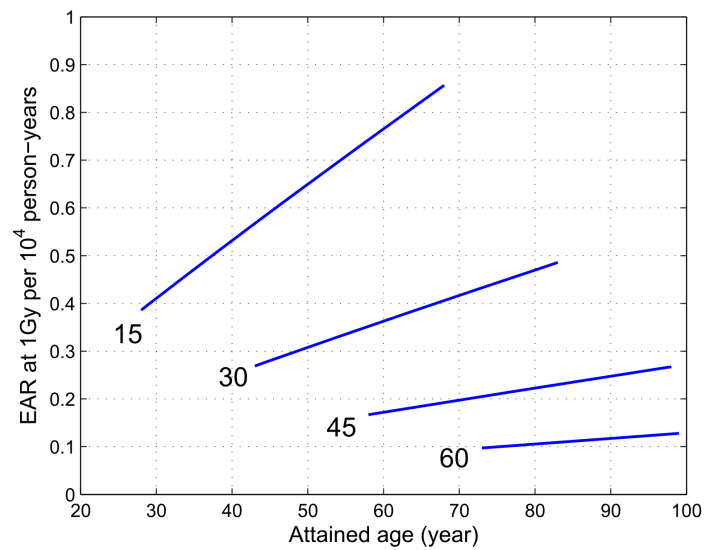
(a) male
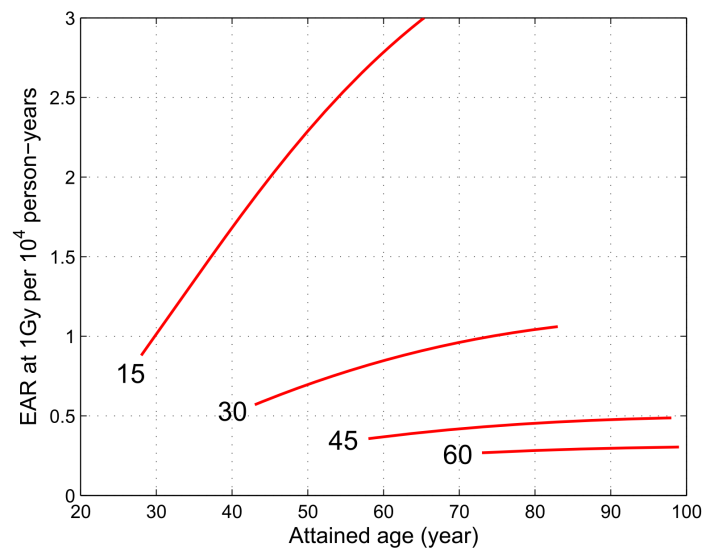
(b) female

Figure 3.4: Excess absolute risk of thyroid cancer after exposure at various ages (shown by numbers) to dose 1 Gy for males (a) and females (b) as estimated using the model of Jacob et al. (2014a)

4 Risk of lung cancer (ICD10:C33,C34) after exposure to radon

Model describing risk of lung cancer after exposure to low-LET radiation had been implemented during the first phase of the ProZES development (Jacob et al., 2013) and is based on the models suggested by Furukawa et al. (2010) and Preston (2011). During the second phase, this model has been complemented by the models describing risk of lung cancer due to exposure to higher-LET radiation originated from inhaled radon and its radioactive progeny.

Radiation exposure of lungs due to inhalation of radon and its radioactive progeny was shown to increase risk of lung cancer as for those exposed occupationally underground, e.g. miners, as for those exposed residentially due to inhalation of radon and its radioactive decay products in the indoor ambient air (BEIR, 1999; Darby et al., 2005; UNSCEAR, 2009; ICRP, 2007; Leuraud et al., 2011; Walsh et al., 2015).

Quantifying an effect of radiation exposure due to radon and its progeny commonly appears as a difficult task due to complicated processes of radon effluence, build-up of radioactive progeny, transport in the atmosphere and in dwellings, chemical forms and attachment to aerosols, intake, deposition and retention of radon-related radioactivity in the human body. Not surprisingly, the dosimetric approach currently adopted by ICRP for radon (ICRP, 1993, 2010, 2014) does not operate with conventional dose units, Gy or Sv, but instead an *ad hoc* unit, called "working level month" (WLM), which represents a cumulative exposure from breathing an atmosphere at certain potential alpha-energy concentration, called "working level" (WL), for a working month of 170 h. Generally, the relationship between exposure in WLM and radiation dose expressed in conventional dosimetric units is conditional on numerous circumstances and assumptions, including equilibrium and attached fractions, aerosol size distribution, inhalation rate, deposition of particles in airways and lungs, absorption, re-distribution and retention of radioactive materials in the body. Although, ICRP declared intentions to use conventional biokinetic and dosimetric techniques for exposures to radon and its progeny (ICRP, 2010), at the time of writing this report, the data for radon are still planned to appear in the third volume of the new compilation of dose coefficients for occupational intake of radionuclides, the first volume of which has already been published (ICRP, 2015).

For estimating risk of lung cancer after occupational underground exposure to radon and its radioactive progeny the recent model of BfS (Kreuzer et al., 2015) has been selected for ProZES. This choice has been justified by the fact that in Germany most of compensation claims emerge from people worked in uranium mines (employees of Wismut AG, also known as the Wismut cohort) and, correspondingly, the radiation risk model built for the same cohort appeared as the most appropriate one for implementation in ProZES. Moreover, the Wismut cohort is the world largest epidemiological cohort of people occupationally exposed to radon, which additionally justifies the model selection.

Table 4.1: Parameters of the model of radiation risk after occupational exposure to radon (Kreuzer et al., 2015)

Parameter	Unit	MLE	σ	95%CI
β_1	none	-4.635	0.235	$(-5.096; -4.174)^a$
β_2	yr^{-1}	-0.0251	0.0066	$(-0.0379; -0.0123)^a$
β_3	none	7.650	0.427	$(6.814; 8.486)^a$
β_4	none	-15.57	4.67	$(-2472; -6.41)^a$
β_5	yr	60^b	—	—
β_6	WLM^{-1}	0.0130	0.0033	$(0.0072; 0.0206)^c$

[a] Wald-type CI

[b] optimised separately (manual fit)

[c] log-likelihood profile-based CI

The BfS model selected for ProZES is based on a sub-cohort of the Wismut miners hired since 1960. This sub-cohort is a relevant group for potential future compensation claims. The exposure assessment in this sub-cohort is of high-quality, because after 1960 the exposure assessment of radon was based on extensive ambient measurements compared to expert ratings in the early years. Because the members of this sub-cohort are still relatively young, effect modification by time since exposure could not be finally evaluated. Therefore, in the current BfS model effect modification by time since exposure is not considered and, correspondingly, calculations of probability of causation are only valid for cases hired since 1960 and being diagnosed at most 15 years after the last exposure. It is anticipated that the effect modification by time since exposure will be considered in the next version of the BfS model when the cohort data will be updated with the new results from the extended follow-up.

The BfS model selected for ProZES was developed by Kreuzer et al. (2015) using non-parametric and parametric baseline rates, the latter one, in the variant suggested in August 2015 (Fenske, 2015), has been included in ProZES and is described below (see Table 4.1).

The fitted parametric baseline has the following form:

$$\lambda_0 = \exp\left[\beta_1 + \beta_2\,(cy - 1973) + \beta_3 \ln\frac{a}{70} + \beta_4 \max^2\left(0, \ln\frac{a}{\beta_5}\right)\right] \tag{4.1}$$

and the radiation risk, defined in terms of ERR, was found as a simple function of the cumulative exposure:

$$ERR = \beta_6\,D(WLM) \tag{4.2}$$

without any other significant effect modifiers.

Besides of mining, exposure to radon and its progeny can be inherent part of other occupational activities: oil and gas exploration, tunnel works, spa and wellness, indoor occupational etc (UN-SCEAR, 2009, Annex E). To assess radiation risk of occupational indoor exposure to radon, the model of Darby et al. (2005) for residential radon exposure has been selected. In this model, no dose

or derived exposure units (e.g. WLM) are used. Instead, indoor air activity concentration (Bq m^{-3}) of parent radon serves to quantify radiological impact. According to Darby et al. (2006, Table B15), the average home occupancy among cases in the study was approximately 60%. Correspondingly, the excess relative risk value reported in this study (0.16 per 100 Bq m^{-3}) is attributed to 30 years of residential exposure to radon in air at concentration 100 Bq m^{-3} with average indoor occupancy 60%, which corresponds to the cumulative exposure time 157788 hours. In ProZES, this model is used to assess radiation risk from occupational exposures to radon. Correspondingly, required input includes both the average radon activity concentration in air q (Bq m^{-3}) and the duration of indoor exposure T (hours)[1]. Then, excess relative risk of lung cancer after radon exposure can be estimated as follows:

$$ERR = \beta_m q \frac{T}{30 \cdot 365.25 \cdot 24 \cdot 0.6} = \frac{\beta_m q T}{157788}, \tag{4.3}$$

where $\beta_m = 1.6$ kBq^{-1} m^3 is the risk coefficient from (Darby et al., 2005) with 95% confidence interval (0.5–3.1) kBq^{-1} m^3. Finally, the following equation is used in ProZES to compute excess relative risk for indoor exposure to radon and progeny:

$$ERR = \beta q T, \tag{4.4}$$

where parameter β is sampled from Gaussian distribution with the following parameters:

$$\mu(\text{Bq}^{-1}\,\text{m}^3\,\text{h}^{-1}) = 1.01 \cdot 10^{-8} \text{ and } \sigma(\text{Bq}^{-1}\,\text{m}^3\,\text{h}^{-1}) = 0.42 \cdot 10^{-8}. \tag{4.5}$$

---

[1] For example, an average annual working time in Germany in the period 2000–2014 accounted for approximately 1408 hours (OECD.stat, https://stats.oecd.org/Index.aspx?DataSetCode=ANHRS)

5 Radiation risk of other solid cancers

5.1 Grouping compatible diseases

During the ProZES development, the models for the most frequent cancers of colon, stomach, lung, and female breast had been developed and implemented in the first version of the software tool (Jacob et al., 2013). These models have been complemented in the second phase by the model for thyroid cancer, which was found to be compatible to risk of thyroid cancer estimated for populations exposed to radioiodine after the Chernobyl accident (more on this see in Chapter 3). Additionally, the group of models based on the LSS cohort (Furukawa et al., 2010) and representing radiation risk of lung cancer after exposure mainly to low-LET radiation have been complemented by the models quantifying radiation risk due to exposure to high-LET radiation of inhaled radon and its progeny (see Chapter 4).

The LSS cohort data also provide information on cancers of other organs. The available cancer incidence data for members of the LSS cohort for the follow-up period from 1958 to 1998 (Preston et al., 2007) have been analysed in order to define appropriate models of radiation risk for remaining types of malignancies. These remaining cancers are generally less frequent and the number of cases for various diagnoses spans from tens to hundreds, not exceeding 1000 cases. An exemption is cancer of liver with 1494 cases in the LSS cohort but cancer of liver is often related to another malignancy, so differentiation between primary and secondary liver malignancies is not always straightforward[1].

A decision was made to aggregate different diagnoses into several functional groups to allow for risk modelling with better statistical significance and reduced uncertainty. The separate diagnoses have been grouped based on their compatibility (functional similarity) to assure for the sufficient number of cases in every group. Additionally, the diseases selected for merging in the same group have been checked for compatibility of their baselines rates in Japanese (source) and German (target) populations. For this, population-specific baseline rates in the source and the target populations for the diseases to be combined in the same group have been compared to check for compatibility of their time trends ("calender year effect") and of their shapes expressed via normalised relative age-dependency. Plots showing comparisons of relative age-dependency of incidence rates for various cancer diagnoses can be found in Appendix 1. The comparison have been performed using cancer incidence data from contemporary population cancer registers in Japan (NCC, 2013) and Germany (RKI, 2013).

As a result of the analysis, the remaining cancer diagnoses have been split into eight groups (see Table 5.1): cancers of digestive (DIG), urinary (URI), male (GNM) and female (GNF1, GNF2)

---

[1]It was noted in a publication on cancer incidence in the LSS cohort in 1959–1998 (Preston et al., 2007) that "The low histological verification rate (41%), the high proportion of DCO cases (21%)..., and the fact that the liver is the common metastatic site are indicative of the difficulties faced in obtaining high-quality data on liver cancer."

genital organs, brain and central nervous system (BCNS), non-melanoma skin cancer (SKIN), and cancers of the remaining (REM) organs. The diagnoses, their ICD10 and the LSS database codes, and the number of cases in the considered LSS dataset are shown in the following Table 5.1.

Table 5.1: Grouping of solid cancers data for the LSS cohort to fit the risk models

Model	Organ or organ group	ICD10 code	LSS code	Cases
DIG (cancers of digestive tract, excluding stomach and colon)				4083
	oral cavity	C00–C14	oralca	277
	oesophagus	C15	esoph	352
	small intestine	C17	smallint	24
	rectum	C19–C21	rectum	838
	liver	C22	liver	1494
	gallbladder, other biliary	C23,C24	gallbldr	549
	pancreas	C25	pancr	512
	other digestive (incl. spleen C26.1)	C26,C48	othdig	37
REM (cancer of remaining organs)				324
	nasal cavity, middle ear, access. sinuses)	C30,C31	nasal	82
	larynx	C32	larynx	133
	thymus	C37	thymus	12
	other respiratory and intrathoracic	C38–C39	othres	27
	bone	C40,C41	bone	20
	connective tissue	C47,C49	connect	33
	testes	C62	testis	17
SKIN (non-melanoma skin cancer)				330
	skin	C44	nmskin	330
GNF1 (cancer of female genital organs, subgroup 1)				978
	uterus, cervix	C53	cervix	859
	uterus, not specified (NOS)[a]	C55	utrnos	119
GNF2 (cancer of female genital organs, subgroup 2)				479
	uterus, corpus	C54	corpus	184
	ovaries, other and non-specified	C56,C57	ovary	245
	other female genital cancer	C51,C52,C57,C58	othfem	50
GNM (cancer of male genital organs)				403
	prostate	C61	prost	387
	other male genital	C60,C63	othmale	16
URI (cancers of urinary tract)				741

Table 5.1: Grouping of solid cancers data for the LSS cohort to fit the risk models (cont'd)

Model	Organ or organ group	ICD10 code	LSS code	Cases
	kidney	C64	kidney	167
	renal pelvis and ureter	C65,C66	renal	80
	urinary bladder	C67	bladder	469
	other urinary	C68	othurin	25
BCNS (cancers of brain and central nervous system)				281
	central nervous system (incl. benign tumours)	C70–C72,D32	cnsca	281
STOMACH	stomach	C16	stomach	4730
COLON	colon cancer	C18	colon	1516
LUNG	lung and trachea	C33,C34	lung	1759
BREAST	female breast	C50	breast	1082
THYROID	thyroid	C73	thyroid	471

[a]in the LSS cohort, mostly represented by cervical cancer (see Preston et al. 2007)

5.2 Generic model for fitting grouped solid cancers

Fitting models of radiation risk for the grouped diagnoses was performed using a common generic phenomenological model framework. Within the framework, for every diagnose group all possible effect modifiers have been tested and only the statistically significant ones were left in the models. Here, the generic model framework used to fit aggregated cancer data of the LSS cohort is described in detail.

The aggregated LSS cohort data represent the number of cancer cases and person-years observed in categorical cells (also called Poisson cells) obtained by stratification of the individual data depending on gender, attained age, age at exposure, dose, and diagnose. Therefore, the expected number of cases in a Poisson cell i can be represented by a product of cell-average incidence rate and the number of person-years observed in the given cell:

$$C_i = \lambda_i PY_i. \tag{5.1}$$

The incidence rate is expressed via baseline rate λ_0, risk function, and (possibly) screening factor, which accounts for time-dependent screening in the LSS cohort due to periodical medical examinations and the autopsy program, which was most actively run in the period before 1970 (Hayashi et al., 2010). Correspondingly, the incidence rate in the exposed cohort can be represented using either excess absolute risk (EAR) or excess relative risk (ERR):

$$\lambda = \begin{array}{ll} \lambda_0\, F_{scr}\,(1+ERR) & \text{for ERR-type risk model} \\ (\lambda_0+EAR)\, F_{scr} & \text{for EAR - type risk model} \end{array} \tag{5.2}$$

5 Radiation risk of other solid cancers

The following general form of the baseline incidence rate was used for fitting:

$$
\begin{aligned}
\lambda_0 = \exp \Big[\ & \beta_1 + \beta_2\,s + \beta_3\,c + \beta_4\,IC+ && \leftarrow \text{constant, sex, city, IC} \\
& + (\beta_5 + \beta_6\,s)\ln\frac{a}{a_c} + (\beta_7 + \beta_8\,s)\ln^2\frac{a}{a_c} + && \leftarrow \text{attained age} \\
& + (\beta_9 + \beta_{10}\,s)\frac{b-b_c}{10} + (\beta_{11} + \beta_{12}\,s)\left(\frac{b-b_c}{10}\right)^2 + && \leftarrow \text{birth year} \\
& + (\beta_{13} + \beta_{14}\,s)\max^2\left(0,\ln\frac{a}{\beta_{15}}\right) + && \leftarrow 1^{\text{st}}\text{ spline joint} \\
& + (\beta_{16} + \beta_{17}\,s)\max^2\left(0,\ln\frac{a}{\beta_{18}}\right)\Big]. && \leftarrow 2^{\text{nd}}\text{ spline joint}
\end{aligned}
\tag{5.3}
$$

A functional expression for the risk functions, either ERR or EAR, has been selected using the common mathematical form:

$$
\begin{aligned}
\left.\begin{array}{c}ERR\\EAR\end{array}\right\} = \ & (\beta_{19} + \beta_{20}\,s)\,D^{\beta_{21}+\beta_{22}\,s}\times && \leftarrow \text{dose multiplier and exponent} \\
& \times \exp\Big[\ (\beta_{23} + \beta_{24}\,s)\,D+ && \leftarrow \text{exponential dose dependence} \\
& + (\beta_{25} + \beta_{26}\,s)\ln\frac{a}{a_c} + (\beta_{27} + \beta_{28}\,s)\ln^2\frac{a}{a_c} + && \leftarrow \text{attained age effects} \\
& + (\beta_{29} + \beta_{30}\,s)\frac{e-e_c}{10} + (\beta_{31} + \beta_{32}\,s)\left(\frac{e-e_c}{10}\right)^2\Big] && \leftarrow \text{age at exposure effects}
\end{aligned}
\tag{5.4}
$$

The screening factor reflecting elevated incidence rate due to medical surveillance and the autopsy program, which was most active in 60s (i.e. prior 1970):

$$
F_{scr} = \exp\left(\beta_{33}\,\text{sign}\,(cy - 1970)\right) = \exp\left(\beta_{33}\,\text{sign}\,(a - e - 25)\right)
\tag{5.5}
$$

Indicator (categorical) variables:

$$
s = \begin{array}{ll} -1 & \text{male} \\ +1 & \text{female} \end{array}
\qquad
c = \begin{array}{ll} -1 & \text{Hiroshima} \\ +1 & \text{Nagasaki} \end{array}
\qquad
IC = \begin{array}{ll} 1 & \text{in city} \\ 0 & \text{not-in-city} \end{array}
\tag{5.6}
$$

The group of residents of Hiroshima and Nagasaki, who were not in the city at the time of detonation, are marked in the LSS dataset as NIC group. This group can be considered as a 'true' control group for residents surviving the explosion. Therefore, in the model description a 'in-city' parameters is used as a modifier to the 'true' baseline for members of the NIC group.

The parametric baseline (5.3) includes cohort-specific parameters c and IC, which have no sense for target populations beyond the LSS cohort. So, if the fitted model baseline includes cohort-specific parameters, then these are averaged and represented as a factor to modify the cohort-independent model baseline. Finally, the baseline equation for a target population is represented as a product of the baseline with all cohort-independent explanatory variables and of an averaged factor calculated using the number of cancer cases in groups of the cohort members, stratified according to their residence and in-city status.

5.3 Fitting details

The model parameters have been found by fitting the LSS incidence data (Preston et al., 2007) using Poisson regression. The best fit parameters have been found by minimization of the deviance, computed as negative of log-likelihood for the data. Namely, given the LSS data in Poisson cells can be represented as matrix

$$\mathbf{X} = (\mathbf{s}, \mathbf{c}, \mathbf{NIC}, \mathbf{a}, \mathbf{e}, \mathbf{d}, \mathbf{PY}, \mathbf{C}), \tag{5.7}$$

then the deviance is computed as

$$\mathrm{dev}(\beta, \mathbf{X}) = 2 \sum_{i:C_i \neq 0} \left[C_i \ln \frac{C_i}{\mu_i(\beta, \mathbf{X})} - (C_i - \mu_i(\beta, \mathbf{X})) \right] + 2 \sum_{i:C_i = 0} \mu_i(\beta, \mathbf{X}), \tag{5.8}$$

where

$$\mu_i(\beta, \mathbf{X}) = \lambda_i(\beta, \mathbf{X}) \, PY_i \tag{5.9}$$

is the model-estimated expected number of cases in the ith Poisson cell.

Unconstrained quasi-Newton minimization as implemented in Matlab Optimization Toolbox (Math-Works, 2015) has been used to minimize the deviance/negative log-likelihood (Eq. 5.8). Only significant parameters (P=0.95) have been kept.

Doses for the grouped cancers have been obtained as average of doses for organs coinciding with or anatomically close to organs of interest.

The fitted parameters were independently checked using the EPICURE software tool (Preston et al., 2015) as a part of quality assurance procedures.

The fitted models have been checked for plausibility by comparing age-dependent model baseline rates with cancer incidence observed in the various years in the whole Japan (NCC, 2013) and incidence reported for Hiroshima and Nagasaki (Forman et al., 2014), only. The data for Hiroshima and Nagasaki came from the city cancer registries, so they included cancer cases among the LSS cohort members and can be partly attributed to radiation exposure. However, effect of exposure can be regarded as insignificant because of (a) low values of radiation-attributable fraction (order of per cents, for most cancers) and (b) the fact that the LSS cohort represents only a part of the total population in these cities.

As a result of the comparison, the model baselines confirmed their plausibility by demonstrating good agreement with incidence rates obtained from the population registries for time periods corresponding to the reported follow-up period 1958–1998. The details can be found in Appendix 2.

Despite of a generally good agreement between the model-calculated baseline rates and the incidence rates reported for the cities (Forman et al., 2014), for some cancer groups the model baseline rates display increasing difference from the population data when extrapolate beyond the follow-up period, after 1998. Such discrepancy appears, for example, when the model baseline for digestive cancers among males is extrapolated to years 2000 and 2005 (see Appendix 2, Figs. 1.5 and 1.6). However, model-estimated incidence rates of digestive cancers for females remain plausible regardless on whether the model estimates are extrapolated or not (ibid., Figs. 1.5 and 1.6).

The comparison has also demonstrated that incidence rates for cervical cancer observed in populations after 1995 demonstrate an age dependence strongly differing from one observed at earlier

time(see Appendix 2, Figs. 3.3–3.5). Given the fact that human papilloma virus (HPV) is known to be an important cause of cervical cancer, the intensive screening and prevention (vaccination) actions undertaken in Japan during last decades (Konno et al., 2010; Tsuji, 2009) may be responsible for significant change of prevalence and age distribution of cervical cancer in Japanese society. The model functions used to describe baseline rates are unable to reproduce age dependence pattern observed after 2000 (ibid., Figs. 3.4 and 3.5).

Finally, the full list of risk models implemented in ProZES is given in the following Table 5.3, which displays group names and their internal identifiers as well as diagnoses and their ICD10-codes.

Table 5.3: Risk models implemented in ProZES and corresponding diagnoses

Model name	Model ID	Diagnose	ICD10-code(s)
STOMACH	16	Stomach cancer	C16
COLON	18	Colon cancer	C18
LUNG	34	Lung cancer (incl.trachea)	C33,C34
BREAST	50	Breast cancer	C50
THYROID	73	Thyroid cancer	C73
DIG	101	Cancer of the oral cavity	C00-C14
		Esophageal cancer	C15
		Small intestine cancer	C17
		Rectum cancer	C19-C21
		Liver cancer	C22
		Cancer of gallbladder, etc	C23,C24
		Pancreatic cancer	C25
		Other cancers of the digestive system	C26,C48
REM	102	Cancer of nasal cavity, etc	C30,C31
		Larynx cancer	C32
		Thymus cancer	C37
		Cancer of heart and other intrathoracic organs	C38,C39
		Bone cancer	C40,C41
		Malignant melanoma	C43
		Connective tissue cancer	C45-C47,C49
		Testis cancer	C62
		Adrenal gland cancer	C74
		Cancer of other or unspecified endocrine glands	C75,C76
GNF1	1031	Uterine cancer/cervix	C53
GNF2	1032	Uterine cancer/corpus	C54
		Uterine cancer/NOS	C55
		Ovarian cancer, etc	C56
		Other female genital cancer	C51,C52,C57,C58
GNM	104	Prostate cancer	C61

Table 5.3: Grouping of solid cancers data for the LSS cohort to fit the risk models (cont'd)

Model name	Model ID	Organ or Organ Group	ICD10-code(s)
		Other male genital cancer	C60,C63
URI	105	Kidney cancer	C64
		Renal pelvis & ureter cancer	C65,C66
		Urinary bladder cancer	C67
		Other urinary system cancer	C68
BCNS	106	Cancer of eyes	C69
		Cancer of central nervous system	C70-C72
SKIN	107	Non-melanoma skin cancer	C44
L1	201	Acute lymphoblastic leukemia (ALL)	C91.0
		Prolymphocytic leukemia of B-cell type	C91.3
		Lymphoid leukemia/unspecified	C91.9
L2	202	Hodgkin disease	C81
		Non-Hodgkin disease	C82,C83,C85,C86
		Lymphoma of peripheral and cutaneous T-cell	C84
		Malignant immunoproliferative disease	C88
		Chronic lymphoblastic leukemia (CLL)	C91.1
		Hairy cell leukemia	C91.4
L3	203	Acute myeloid leukemia (AML)	C92.0
		Sub-acute myeloid leukemia	C92.2
		Myeloid sarcoma	C92.3
		Acute promyelocytic leukemia	C92.4
		Acute myelomonocytic leukemia	C92.5
		Monocytic leukemia	C93
		Other leukemia of specified cell type	C94
		Leukemia of unspecified cell type	C95
		Other or non-specified	C96
L4	204	Chronic myeloid leukemia (CML)	C92.1

Table 5.2: Main properties of the models derived from the LSS data for grouped diagnoses

Group	Cases	ERR (Gy⁻¹)			EAR ($10^{-4}\,py^{-1}\,Gy^{-1}$)		
		Attrib. fraction[a] (%)	Constant (p-value)	Power of att. age[b] (p-value)	Attrib. fraction[a] (%)	Constant (p-value)	Power of att. age[b] (p-value)
DIG	4083	2.8	0.24 (0.001)	−3.04 (<0.001)	2.4	6.85 (<0.001)	2.26 (<0.001)
REM	324	4.8	0.25 (0.20)	−2.77 (0.02)	4.5	0.60[c] (0.03)	−
GNF1	978	0.45	0.06 (0.68)	−	0.8	0.57 (0.4)	−
GNF2	479	2.7	0.35 (0.12)	−	1.5	0.49 (0.3)	−
GNM	403	1.1	0.12 (0.56)	−	1.9	0.81 (0.06)	−
		1.6	0.20 (0.37)	−3.7 (0.27)			
URI	741	7.9	1.21[d] (<0.001)	−	7.3	4.19 (<0.001)	3.63 (<0.001)
BCNS	281	5.0	0.23 (0.23)	−2.97 (0.009)	4.1	0.46 (0.046)	−
SKIN	330	11.7	0.71[e,f] (0.018)	−	11.2	1.18[g,h] (0.021)	3.65 (<0.001)

[a] fraction of the observed incidence rate, which is attributable to radiation exposure

[b] centred at attained age 70

[c] gender-averaged value; effect of sex has low significance (p = 0.14) resulting in gender-dependent EAR ($10^{-4}\,py^{-1}\,Gy^{-1}$) 1.0 (males) and 0.2 (females).

[d] gender-averaged value; effect of sex is significant (p = 0.011) and results at age 70 in gender-dependent ERR per 1 Gy ≈0.5 (males) and ≈1.9 (females)

[e] non-linear dose response with dose exponent equal to 1.55 (p <0.001)

[f] 'age-at exposure' effect modifier of log-risk equals to −89% per decade (p <0.001)

[g] non-linear dose response with dose exponent 1.60 (p <0.001)

[h] 'age-at-exposure' effect modifier of log risk equals to −75% per decade (p <0.001)

6 Risk models for digestive cancers (DIG group)

The group DIG combines together cancers of digestive tract organs other than colon and stomach. Namely, cancers of oral cavity (ICD10:C00–C14), oesophagus (ICD10:C15), small intestine (ICD10:C17), rectum (ICD10:C19–C21), liver (ICD10:C22), gallbladder and related organs (ICD10:C23,C24), pancreas (ICD10:C25), and other organs of digestive system (ICD10:C26,C48). For the follow-up period 1958–1998, this group encounters 4083 cancers cases. In ProZES, this group is coded with the group code 101, which should be used in case of manual preparation of input files.

Fitting of the risk functions have been performed with doses computed as arithmetic average of weighted doses for colon, liver, pancreas, and bladder. As seen from Fig. 6.1, the average weighted doses used for the DIG group, despite of some random scatter, agree well with the values of weighted colon doses, as found in the LSS cohort database.

The fitting resulted in two models: one of ERR-type and one of EAR-type. Both models use 14 parameters to characterise baseline and excess rates. Main statistical properties of the fitted models are shown in Table 6.1. The terms and notations used in the model equations below are those of the generic model, which is fully described in Section 5.2.

The EAR-type model (coded in ProZES as DIG-EAR14) contributes to the generated distribution of assigned share Z only 28.7%. For this model, the parametric baseline rate has been defined in the

Table 6.1: Statistical properties of the models fitted to characterize risk of cancers of digestive organs (group DIG) for members of the LSS cohort

Model type (name)	K	Estimated cases		deviance	ΔAIC	AIC-weight (%)
		baseline	excess			
ERR (DIG-ERR14)	14	3970.3	112.7	8030.01	0	71.3
EAR (DIG-EAR14)	14	3983.5	99.5	8031.83	1.82	28.7
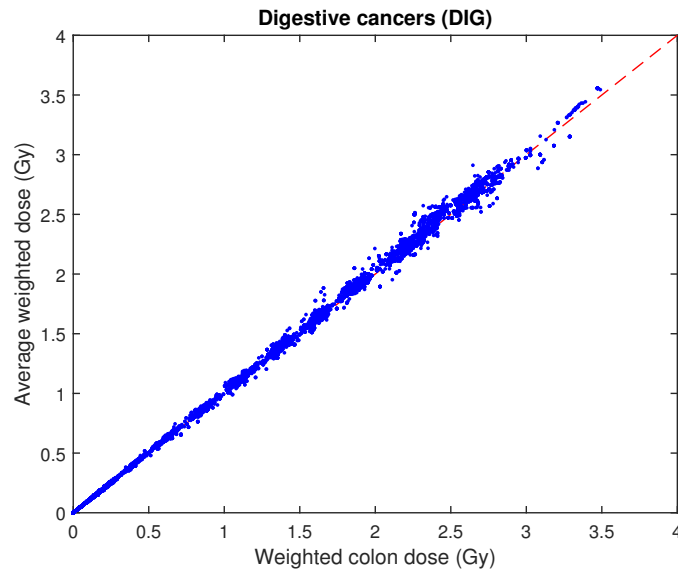
Figure 6.1: Comparison of average weighted dose for the group of digestive cancers with weighted colon dose

following form:

$$\lambda_0(10^{-4} PY^{-1}) = \exp\left[\beta_1 + \beta_2 s + \beta_4 IC + (\beta_5 + \beta_6 s) \ln \frac{a}{70} + \beta_8 s \ln^2 \frac{a}{70} + \right.$$

$$+ (\beta_9 + \beta_{10} s) \frac{b - 1915}{10} + (\beta_{11} + \beta_{12} s) \left(\frac{b - 1915}{10}\right)^2 + \tag{6.1}$$

$$\left. + \beta_{13} \max^2 \left(0, \ln \frac{a}{\beta_{15}} \right) \right].$$

Correspondingly, radiation risk (EAR) has been defined with linear dose response and the only modifier dependent on attained age:

$$EAR(10^{-4} PY^{-1}) = \beta_{19} D \exp\left(\beta_{25} \ln \frac{a}{70} \right). \tag{6.2}$$

The ERR-type model (coded in ProZES as DIG-ERR14) dominates in the generated distribution of assigned share Z and contributes 71.3% of the whole generated sample. The parametric form of

Table 6.2: Parameters and parameter statistics for the selected models of the DIG (other digestive cancers) model group

Parameter	ERR-type model (ERR14)			EAR-type model (EAR14)		
	Estimate	(*p*-value)	95%CI	Estimate	(*p*-value)	95%CI
β_1	3.71	(<0.001)	(3.64; 3.88)	3.71	(<0.001)	(3.63; 3.9)
β_2	−0.51	(<0.001)	(−0.57; −0.46)	−0.45	(<0.001)	(−0.48; −0.41)
β_4	0.078	(0.040)	(0.04; 0.15)	0.083	(0.028)	(0.046; 0.16)
β_5	6.88	(<0.001)	(6.63; 7.43)	6.91	(<0.001)	(6.64; 7.5)
β_6	—	—	—	0.66	(<0.001)	(0.52; 0.96)
β_8	0.95	(<0.001)	(0.41; 1.49)	1.91	(<0.001)	(1.24; 2.6)
β_9	−0.25	(<0.001)	(−0.28; −0.22)	−0.25	(<0.001)	(−0.28; −0.22)
β_{10}	0.045	(0.003)	(0.016; 0.073)	0.041	(0.009)	(0.026; 0.072)
β_{11}	0.020	(0.005)	(0.006; 0.033)	0.019	(0.007)	(0.005; 0.033)
β_{12}	−0.020	(0.003)	(−0.033; −0.007)	−0.019	(0.006)	(−0.033; −0.006)
β_{13}	−6.36	(<0.001)	(−8.24; −4.72)	−6.50	(<0.001)	(−8.6; −4.8)
β_{14}	1.64	(<0.001)	(1.16; 3.0)	—	—	—
β_{15}	58.5	(<0.001)	(54; 63.5)	58.7	(<0.001)	(53.4; 64.4)
β_{19}	0.24	(0.001)	(0.17; 0.40)	6.85	(<0.001)	(4.9; 11)
β_{25}	−3.04	(<0.001)	(−3.9; −1.2)	2.26	(<0.001)	(0.93; 3.7)

the baseline rate appears as follows:

$$\lambda_0(10^{-4}\,PY^{-1}) = \exp\left[\beta_1 + \beta_2 s + \beta_4 IC + \beta_5 \ln\frac{a}{70} + \beta_8 s \ln^2\frac{a}{70} + \right.$$
$$+ (\beta_9 + \beta_{10}s)\frac{b-1915}{10} + (\beta_{11} + \beta_{12}s)\left(\frac{b-1915}{10}\right)^2 + \tag{6.3}$$
$$\left. + (\beta_{13} + \beta_{14}s)\max^2\left(0, \ln\frac{a}{\beta_{15}}\right)\right]$$

and the risk function as:

$$ERR = \beta_{19}D\exp\left(\beta_{25}\ln\frac{a}{70}\right). \tag{6.4}$$

The model parameters and their main statistics, including *p*-values and 95% confidence intervals derived from log-likelihood profiles, are given in Table 6.2.

Resulting best estimates of the assigned share for both models and for their MMI-average shown as a function of attained age are compared in the following Figs. 6.2–6.5 for males and females acutely exposed to dose 1 Gy at ages 20 and 50 years. Indicated by solid lines are model estimates corresponding to the time since exposure in range from 13 to 53 years, which reflects the follow-up period of the considered LSS cancer incidence data. Extrapolations beyond this range are shown as
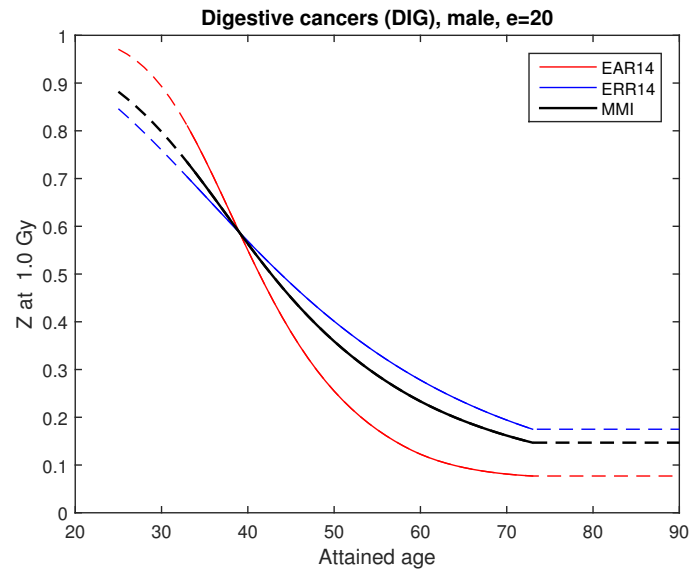
Figure 6.2: Probability of causation for other digestive cancers (DIG group) for male exposed at age 20 as estimated using partial models (blue, red) and their MMI-aggregate (black). Dashed lines indicate extrapolations beyond the LSS cohort-supported range.

dashed lines. Extrapolation to times since exposure shorter than 13 years are done using the estimated model age- and time-dependencies, excluding assumed latency period, while extrapolations beyond 53 years since exposure are done using the fixed values estimated at 53 years after exposure.
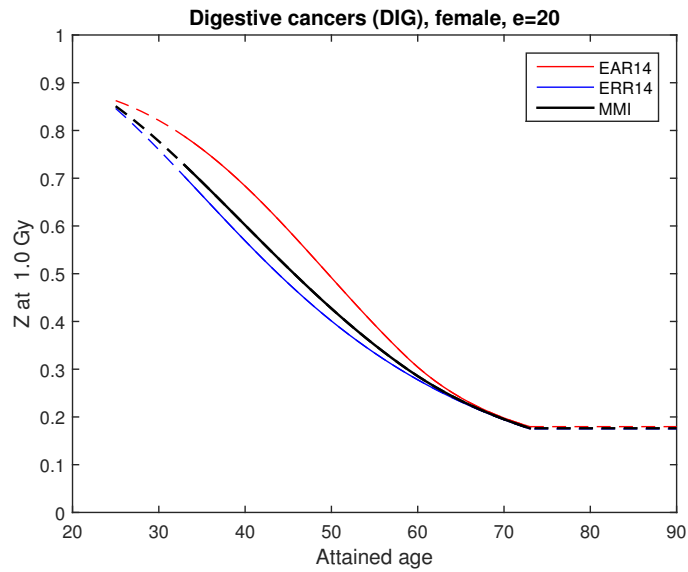
Figure 6.3: Probability of causation for other digestive cancers (DIG group) for female exposed at age 20 as estimated using partial models (blue, red) and their MMI-aggregate (black). Dashed lines indicate extrapolations beyond the LSS cohort-supported range.

Figure 6.4: Probability of causation for other digestive cancers (DIG group) for male exposed at age 50 as estimated using partial models (blue, red) and their MMI-aggregate (black). Dashed lines indicate extrapolations beyond the LSS cohort-supported range.

Figure 6.5: Probability of causation for other digestive cancers (DIG group) for female exposed at age 50 as estimated using partial models (blue, red) and their MMI-aggregate (black). Dashed lines indicate extrapolations beyond the LSS cohort-supported range.

7 Cancer of urinary tract organs (URI group)

The group URI combines together cancers of urinary system organs: kidneys (ICD10:C64), renal pelvis and ureter (ICD10: C65,C66), urinary bladder (ICD10:C67), and other parts of urinary tract (ICD10:C68). In the LSS cohort, there are 741 cancer cases of these diagnoses. In ProZES, an internal code value 105 is defined for the URI group of diagnoses. This internal code should be used during manual editing of the input files to specify diagnoses belonging to the URI group.

Fitting was performed with doses calculated as arithmetic average of weighted absorbed doses for colon, liver, and bladder. Comparison shows (see Fig. 7.1) that the average doses for group URI are very similar to, although not exactly the same as, the weighted colon doses.

Fitting the LSS data ended up with two best models: a winner model of EAR-type (AIC-weight 53%) and another model of ERR-type (AIC-weight 47%). The models have 10 and 9 parameters, correspondingly, and are designated in ProZES as models URI-EAR10 and URI-ERR9. The main statistics of these models' fit is represented in Table 7.1. The terms and notations used in the model equations below are those of the generic model, which is fully described in Section 5.2.

The ERR-type model (attributable fraction 7.9%) has parametric baseline in the following form:

$$\lambda_0(10^{-4} PY^{-1}) = \exp\left[\beta_1 + \beta_2 s + \beta_5 \ln\frac{a}{70} + \right.$$
$$\left. + \beta_9 \frac{b-1915}{10} + \beta_{11}\left(\frac{b-1915}{10}\right)^2 + \beta_{13}\max^2\left(0, \ln\frac{a}{\beta_{15}}\right) \right] \tag{7.1}$$

and risk, represented as ERR, in the following form:

$$ERR = (\beta_{19} + \beta_{20}s)D. \tag{7.2}$$

Table 7.1: Statistical properties of the models fitted to characterize risk of cancers of urinary tract organs (group URI) for members of the LSS cohort

Model type (name)	K	Estimated cases		Deviance	ΔAIC	AIC weight (%)
		baseline	excess			
ERR (URI-ERR9)	9	682.3	58.7	3368.67	0.24	47.0
EAR (URI-EAR10)	10	687.0	54.0	3366.43	–	53.0
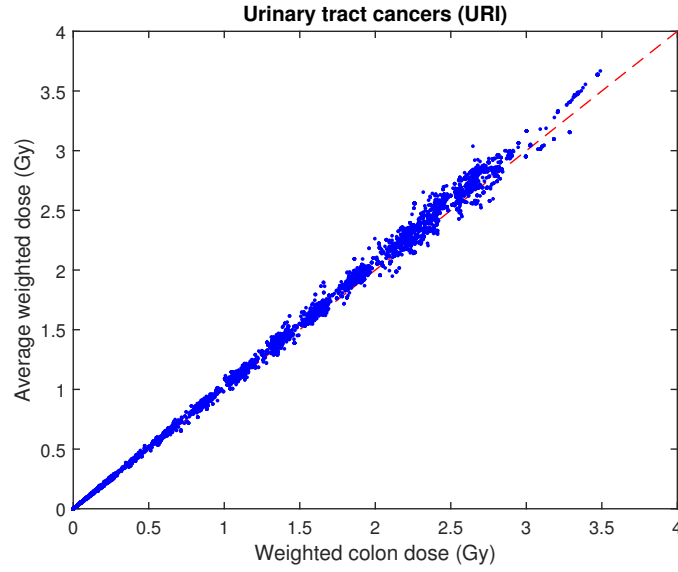
Figure 7.1: Comparison of average weighted dose for the group of urinary cancers with weighted colon dose

The EAR-type model (attributable fraction 7.3%) has parametric baseline in the following form:

$$\lambda_0(10^{-4}PY^{-1}) = \exp\left[\beta_1 + \beta_2 s + \beta_5 \ln\frac{a}{70} + \beta_7 \ln^2\frac{a}{70} + \right.$$
$$\left. +\beta_9\frac{b-1915}{10} + \beta_{11}\left(\frac{b-1915}{10}\right)^2 + \beta_{13}\max^2\left(0, \ln\frac{a}{\beta_{15}}\right)\right] \quad (7.3)$$

and the risk, expressed as EAR, as:

$$EAR(10^{-4}PY^{-1}) = \beta_{19}D\exp\left(\beta_{25}\ln\frac{a}{70}\right). \quad (7.4)$$

The models of radiation risk selected for the group of urinary organ cancers are almost equally represented in the MMI-aggregated estimate of assigned share Z: 47% for the ERR-type model and 53% for the EAR-type one. Baseline incidence rates according to the both models agree well with observed rates for cancers of the urinary group in Hiroshima and Nagasaki not only in the period from 1975 to 1995, i.e. within the LSS cohort follow-up time, but also for later years after 1995. Calender year effect in the baseline is not strong, thus model baseline rates fixed at 53 years after exposure and extrapolated beyond describe incidence from population registers almost equally good (see Section 5 in the Appendix 2). Comparison of estimates of assigned share from the models and their MMI-weighted average are shown in Figs. 7.2–7.5. In the figures, extrapolation beyond the range supported by the LSS follow-up data is indicated by dashed lines (see details in Chapter 6).

Table 7.2: Parameters and parameter statistics for the selected models of the URI (cancers of urinary tract organs) model group

Parameter	ERR-type model (URI-ERR9)			EAR-type model (URI-EAR10)		
	Estimate	(p-value)	95%CI	Estimate	(p-value)	95%CI
β_1	1.80	(<0.001)	(1.72; 1.98)	2.25	(<0.001)	(1.9; 3.7)
β_2	−0.66	(<0.001)	(−0.75; −0.58)	−0.66	(<0.001)	(−0.74; −0.58)
β_5	7.07	(<0.001)	(6.65; 8.0)	10.6	(<0.001)	(8.8; 14)
β_7	—	—	—	4.1	(0.018)	(0.72; 4.4)
β_9	−0.26	(<0.001)	(−0.33; −0.19)	−0.29	(<0.001)	(−0.36; −0.21)
β_{11}	0.033	(0.035)	(0.002; 0.063)	0.040	(0.017)	(0.007; 0.072)
β_{13}	−14.6	(0.015)	(−26.3; −6.6)	−13.4	(<0.001)	(−19; −7.7)
β_{15}	69.6	(<0.001)	(62.3; 76.8)	58.6	(<0.001)	(49.3; 72)
β_{19}	1.21	(<0.001)	(0.94; 1.85)	4.2	(<0.001)	(3.2; 6.4)
β_{20}	0.73	(0.011)	(0.45; 1.36)	—	—	—
β_{25}	—	—	—	3.6	(<0.001)	(2.7; 5.7)

Figure 7.2: Probability of causation for urinary cancers (URI group) for male exposed at age 20 as estimated using partial models (blue, red) and their MMI-aggregate (black). Dashed lines indicate extrapolations beyond the LSS cohort-supported range.
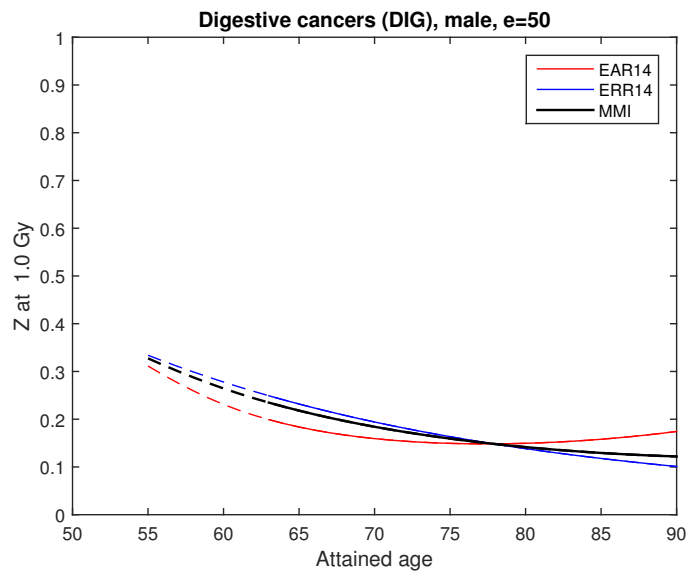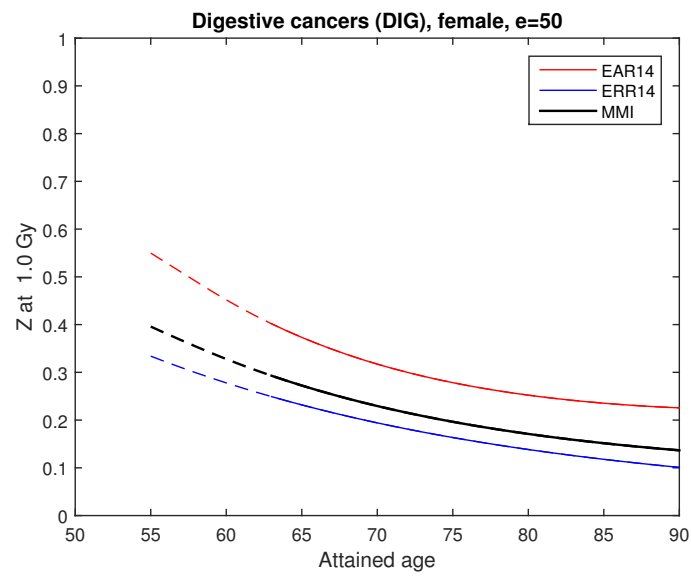
Figure 7.3: Probability of causation for urinary cancers (URI group) for female exposed at age 20 as estimated using partial models (blue, red) and their MMI-aggregate (black). Dashed lines indicate extrapolations beyond the LSS cohort-supported range.

Figure 7.4: Probability of causation for urinary cancers (URI group) for male exposed at age 20 as estimated using partial models (blue, red) and their MMI-aggregate (black). Dashed lines indicate extrapolations beyond the LSS cohort-supported range.

Figure 7.5: Probability of causation for urinary cancers (URI group) for female exposed at age 50 as estimated using partial models (blue, red) and their MMI-aggregate (black). Dashed lines indicate extrapolations beyond the LSS cohort-supported range.

8 Female genital organs

The models for female genital organs have been fit using uterus dose for cervical cancer and average of the uterus, ovaries, and bladder doses for cancers of other female genital organs. Analysis of baseline incidence rates in Japan has shown that age-dependence of cervical cancer differs substantially from that for other uterus, ovaries and other genital organs. For example, baseline incidence rate of cervical cancer in Japan in 2010 (NCC, 2012) shows increase starting age 25, peaked at age 40, and reduced two times at age 70. Other female genital cancers show different shape: starting after age 35, peaking at age 60, and dropping down two times at age 80 (see Appendix 1).

Patterns of age dependency for cancers of cervix, other uterus and ovaries have been compared for time period from 1975 to 2005. The comparison has shown that relative age-dependence of cervical cancer is hardly compatible with that for cancers of other female genital organs. This discrepancy had justified splitting of the female genital cancer group into two groups and modelling them independently.

Fitting models of radiation-attributed risk has been conducted with the LSS incidence data. As indicated by Preston et al. (2007), the group of non-specified uterine cancers (LSS code 'utrnos') consists mostly of cervical cancers, thus these cases have been added to cervical ones and analysed together. Observed in the LSS cohort cases of cancers of uterine corpus, ovary and other female genital organs have created the second group to fit.

8.1 Cervical cancer (GNF1 group)

Fitting cervical cancers in the LSS cohort was performed using weighted doses for uterus, which appears very similar to the weighted colon dose, as seen in Fig. 8.1.

The group GNF1 combined together 978 cancer cases, of which 859 were reported as of cervical type in the LSS dataset. The rest 119 cases were marked as 'uterus, NOS' but according to Preston et al. (2007) most of the cancers marked as 'non-specified' were of cervical type, too. This justified combining these two diagnoses in the LSS dataset into the same group for fitting. For internal use in ProZES and for coding diagnosis during manual preparation of input data, the group was indicated with the code number 1031.

Fitting of the data resulted in two models: one of ERR-type and another of EAR-type. These fitted models are indicated as GNF1-EAR8 and GNF1-ERR8 and their main statistical properties are shown in Table 8.1. The models provide approximately equal statistical quality and, correspondingly, make similar contributions to MMI-based estimates: $\approx 57\%$ from EAR-type model and the rest, $\approx 43\%$, from the ERR-type one. The terms and notations used in the model equations below are those of the generic model, which is fully described in Section 5.2.
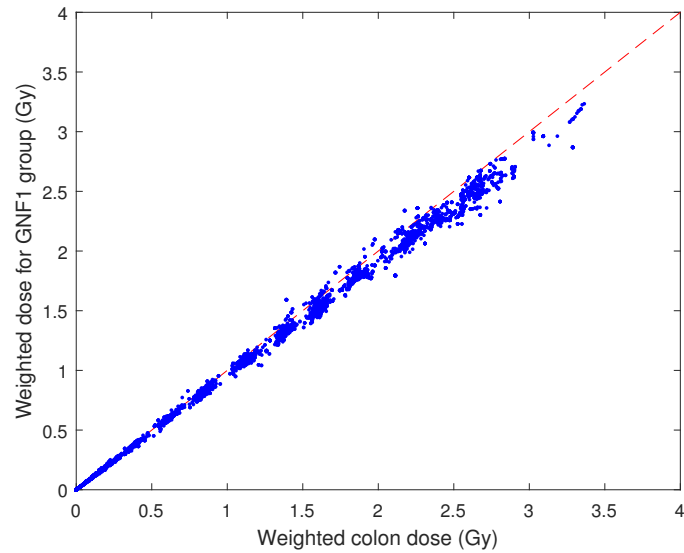
Figure 8.1: Comparison of average weighted dose for cervical cancers (group GNF1) with weighted colon dose

Table 8.1: Statistical properties of the models fitted to characterize risk of female cervical cancers (group GNF1) for members of the LSS cohort

Model type (name)	K	Estimated cases: baseline	excess	Deviance	ΔAIC	AIC-weight (%)
EAR (GNF1-EAR8)	8	970.0	8.0	2861.05	–	57.08
ERR (GNF1-ERR8)	8	973.6	4.4	2861.62	0.57	42.92

Table 8.2: Parameters and parameter statistics for the selected models of the GNF1 (cervical cancer) model group

Parameter	ERR-type model (GNF1-ERR8)			EAR-type model (GNF1-EAR8)		
	Estimate	(*p*-value)	95%CI	Estimate	(*p*-value)	95%CI
β_1	0.91	(0.11)	$(-1.3; 1.64)$	0.75	(0.23)	$(-4.1; 1.6)$
β_5	-5.92	(0.006)	$(-8.0; -3.0)$	-6.62	(0.007)	$(-9.0; -3.3)$
β_7	-6.69	(<0.001)	$(-10.4; -3.9)$	-7.40	(0.001)	$(-11.9; -4.1)$
β_9	0.34	(<0.001)	$(0.31; 0.41)$	0.35	(<0.001)	$(0.32; 0.41)$
β_{11}	-0.030	(0.034)	$(-0.057; -0.003)$	-0.031	(0.031)	$(-0.058; -0.003)$
β_{13}	6.52	(0.002)	$(4.4; 11.6)$	7.27	(0.005)	$(4.7; 14.6)$
β_{15}	48.5	(<0.001)	$(40.5; 60)$	48.0	(<0.001)	$(35.5; 59)$
β_{19}	0.06	(0.68)	$(-0.08; 0.35)$	0.57	(0.41)	$(-0.11; 2.0)$

The fitted models share the similar parametric representation for the model baselines:

$$
\lambda_0(10^{-4}PY^{-1}) = \exp\left[\beta_1 + \beta_5 \ln\frac{a}{70} + \beta_7 \ln^2\frac{a}{70} + \right.
$$
$$
\left. + \beta_9 \frac{b-1915}{10} + \beta_{11}\left(\frac{b-1915}{10}\right)^2 + \beta_{13}\max^2\left(0, \ln\frac{a}{\beta_{15}}\right) \right], \tag{8.1}
$$

and simplest linear-dose-response representations for radiation risk:

$$
EAR(10^{-4}PY^{-1}) = \beta_{19}D \tag{8.2}
$$

for excess absolute risk and

$$
ERR = \beta_{19}D \tag{8.3}
$$

for excess relative risk. The model parameters and their statistics are given in Table 8.2, where MLE estimates along with their *p*-values and profile log-likelihood-based confidence intervals are shown.

Both risk models (ERR- and EAR-type) are simple, without any effect modifiers. Both risk estimates are of low significance (high *p*-values). This can be attributed to large variations of baseline, including strong non-linear time trend. Human papilloma virus (HPV) is recognized as a contagion of cervical cancer and has strong impact on incidence among other risk factors. HPV and other risk factors result in increase of baseline incidence rate and reduce relative contribution of radiation-related cervical cancers. This could explain small and low-significant values of estimated risk (both ERR and EAR).

The cervical cancer baseline in Japan, including Hiroshima and Nagasaki cities, is strongly affected by screening and prevention (vaccination) actions taken during the last decades (Tsuji, 2009; Konno et al., 2010). These apparently result in non-standard age- and time-dependencies of the baseline. The selected model structure cannot adequately address such changes in the baseline, so it is
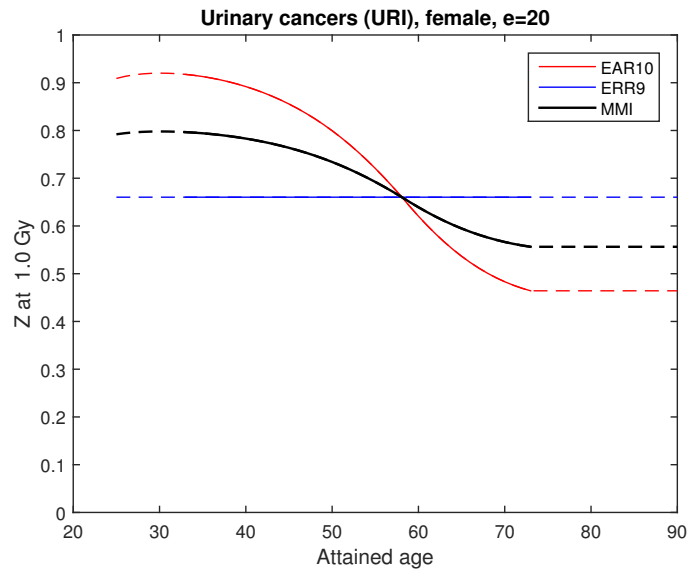
Figure 8.2: Probability of causation for cervical cancers (GNF1 group) for female exposed at age 20 as estimated using partial models (blue, red) and their MMI-aggregate (black). Dashed lines indicate extrapolations beyond the LSS cohort-supported range.
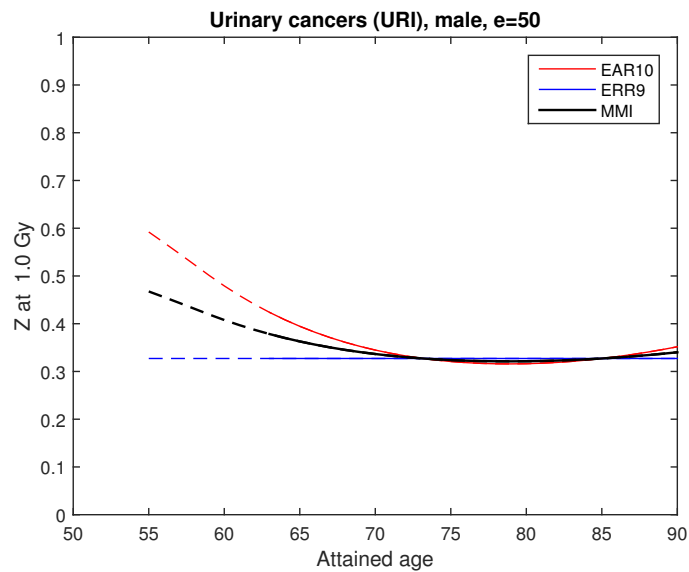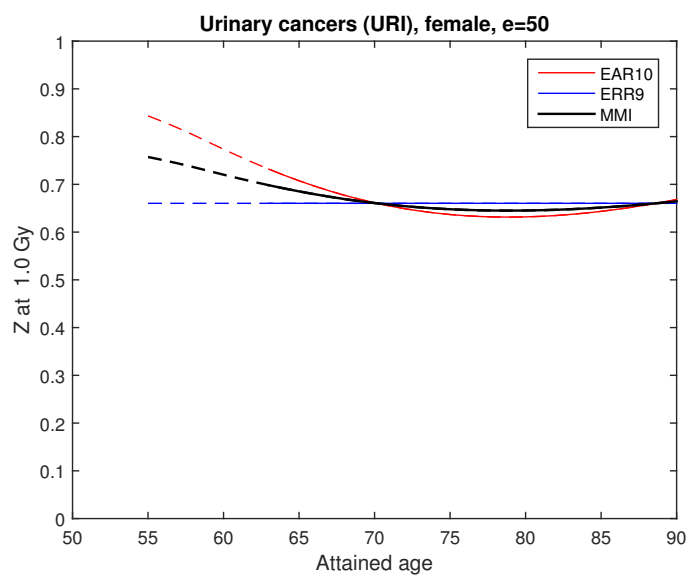
not unlikely that better description and more significant risk estimates might be obtained with model having another structure. Though, such (re)analysis would be advisable when the new LSS data for the extended follow-up period will become available.

Small fitted risk values result in small values of radiation-assigned share of probability of cervical cancer (see Figs. 8.2–8.4). In the figures, extrapolation beyond the range supported by the LSS follow-up data is indicated by dashed lines (see details in Chapter 6).

8.2 Other female genital cancers (GNF2 group)

The group included 479 cancer cases, of which 184 were cancers of uterus (corpus, ICD10:C54), 245 were ovarian cancers (ICD10:C56,C57), and 50 cases were cancers of other female genital organs, including external ones (ICD10:C51,C52,C57,C58). For manual preparation of the input data, this group is designated by an internal code 1032.

Fitting of the GNF2 group models was performed using average dose response for uterus, ovaries, and bladder. The weighted dose for the GNF2 group agrees well with the weighted colon dose (see Fig. 8.5).

Fitting of the data resulted in two models: one of ERR-type and another of EAR-type (see Table 8.3), Correspondingly, these models are designated as GNF2-EAR5 and GNF2-ERR5. The terms and notations used in the model equations below are those of the generic model, which is fully described in Section 5.2.

Figure 8.3: Probability of causation for cervical cancers (GNF1 group) for female exposed at age 35 as estimated using partial models (blue, red) and their MMI-aggregate (black). Dashed lines indicate extrapolations beyond the LSS cohort-supported range.
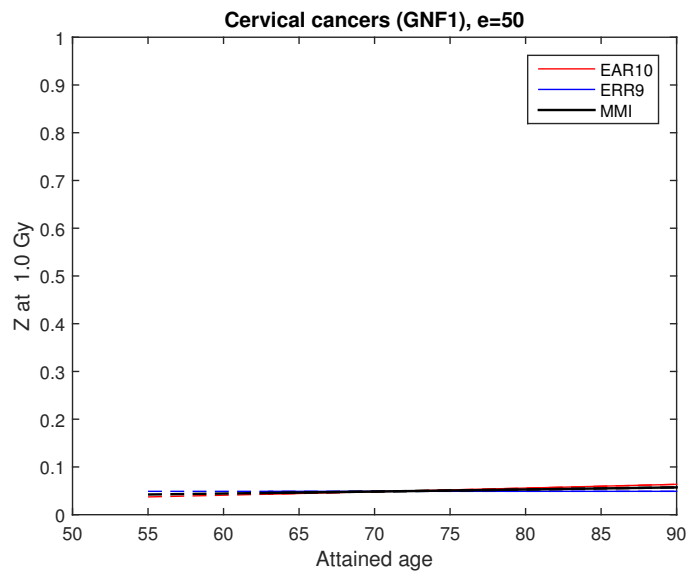
Figure 8.4: Probability of causation for cervical cancers (GNF1 group) for female exposed at age 50 as estimated using partial models (blue, red) and their MMI-aggregate (black). Dashed lines indicate extrapolations beyond the LSS cohort-supported range.
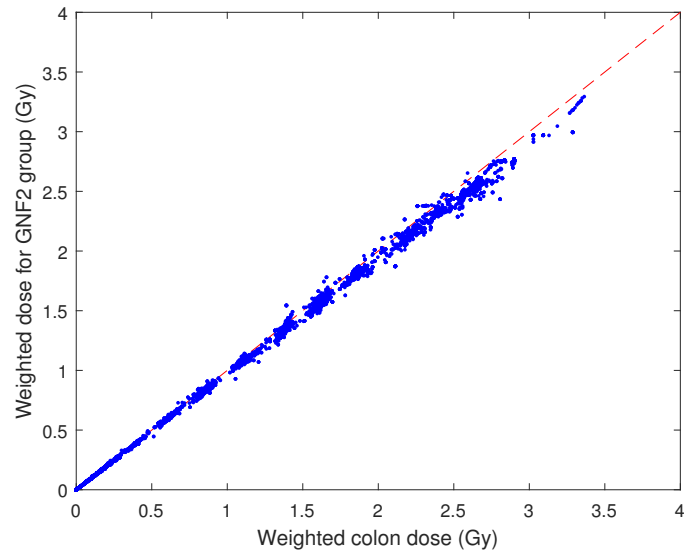
Figure 8.5: Comparison of average weighted dose for the female genital cancers other than cervical one (group GNF2) with weighted colon dose

Table 8.3: Statistical properties of the models fitted to characterize risk of female cancers of genital organs (group GNF2) for members of the LSS cohort

Model type (name)	K	Estimated cases: baseline	excess	Deviance	ΔAIC	AIC-weight (%)
EAR (GNF2-EAR5)	5	472.0	7.0	1970.87	1.93	27.59
ERR (GNF2-ERR5)	5	465.9	13.1	1969.11	—	72.41

Table 8.4: Parameters and parameter statistics for the selected models of the GNF2 group (female genital organs, excluding cervix uteri)

Parameter	ERR-type model (GNF2-ERR5)			EAR-type model (GNF2-EAR5)		
	Estimate	(*p*-value)	95%CI	Estimate	(*p*-value)	95%CI
β_1	1.49	(<0.001)	(1.4; 1.6)	1.51	(<0.001)	(1.4; 1.6)
β_5	1.1	(0.009)	(0.28; 1.9)	1.07	(0.012)	(0.24; 1.9)
β_7	−2.98	(<0.001)	(−4.4; −1.6)	−3.13	(<0.001)	(−4.6; −1.7)
β_9	−0.12	(0.004)	(−0.21; −0.04)	−0.12	(0.005)	(−0.21; −0.04)
β_{19}	0.35	(0.12)	(0.13; 0.86)	0.49	(0.30)	(0.03; 1.6)

The fitted models have the same structure of the parametric baseline, which appear as follows:

$$\lambda_0(10^{-4}PY^{-1}) = \exp\left[\beta_1 + \beta_5 \ln \frac{a}{70} + \beta_7 \ln^2 \frac{a}{70} + \beta_9 \frac{b-1915}{10}\right]. \tag{8.4}$$

Relatively small number of cancer cases in the group GNF2 (479 cases) did not allow to define statistically significant effect modifiers, thus both, EAR- and ERR-type, risk functions have been defined in the simplest form with the only parameter, defining linear dose response of the radiation risk:

$$EAR(10^{-4}PY^{-1}) = \beta_{19} D \tag{8.5}$$

and

$$ERR = \beta_{19} D. \tag{8.6}$$

The model parameters (ML estimates) and their statistics (*p*-values and PLL-based CI) are shown in Table 8.4. As seen from the table, risk-related parameters β_{19} for both models are of low significance ($p > 0.1$), although their significance is somewhat better than that obtained for cervical cancers (group GNF1, see previous section).

Assigned shares computed using the fitted models and their MMI-aggregate for single acute exposures with dose 1 Gy at ages 20, 35, and 50 are shown in the following Figs. 8.6–8.8. In the figures, extrapolation beyond the range supported by the LSS follow-up data is indicated by dashed lines (see details in Chapter 6).
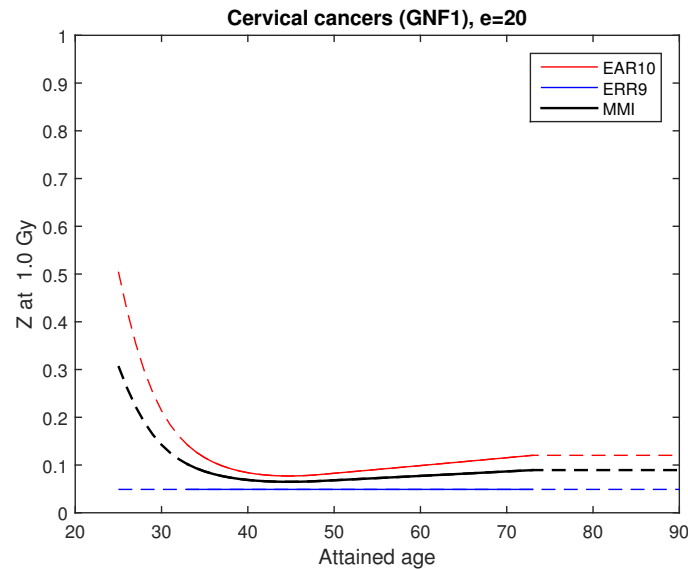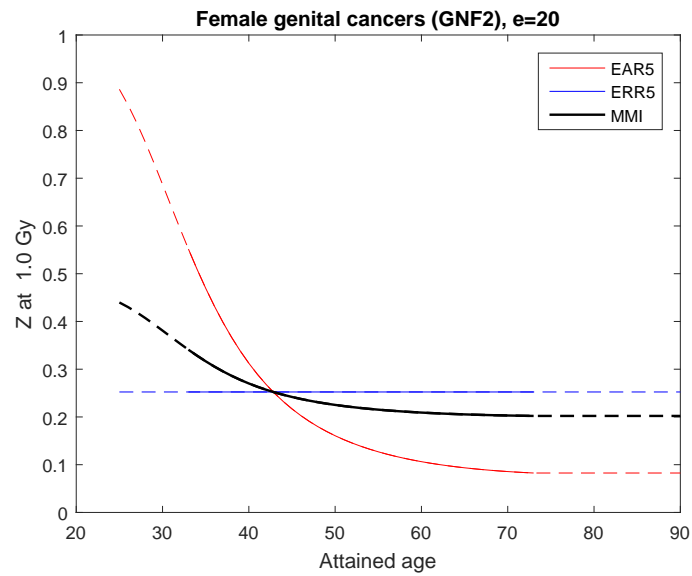
Figure 8.6: Probability of causation for female genital cancers (GNF2 group) for a female exposed at age 20 using estimated partial models (blue, red) and their MMI-aggregate (black). Dashed lines indicate extrapolations beyond the LSS cohort-supported range.
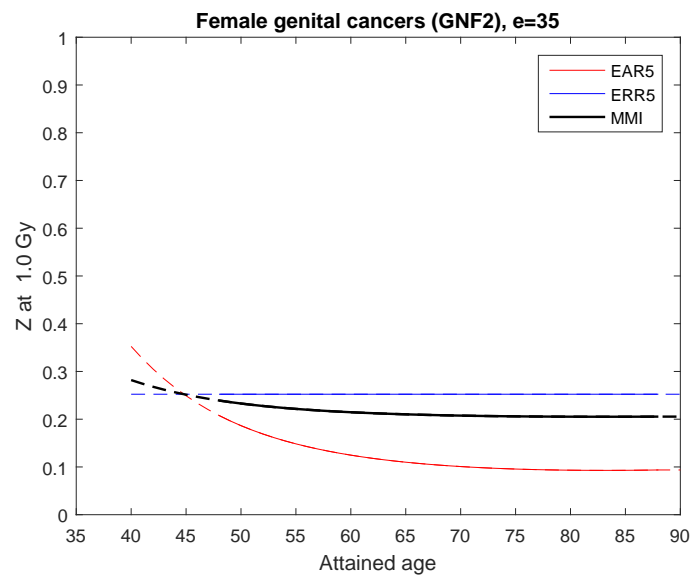
Figure 8.7: Probability of causation for female genital cancers (GNF2 group) for female exposed at age 35 using estimated partial models (blue, red) and their MMI-aggregate (black). Dashed lines indicate extrapolations beyond the LSS cohort-supported range.
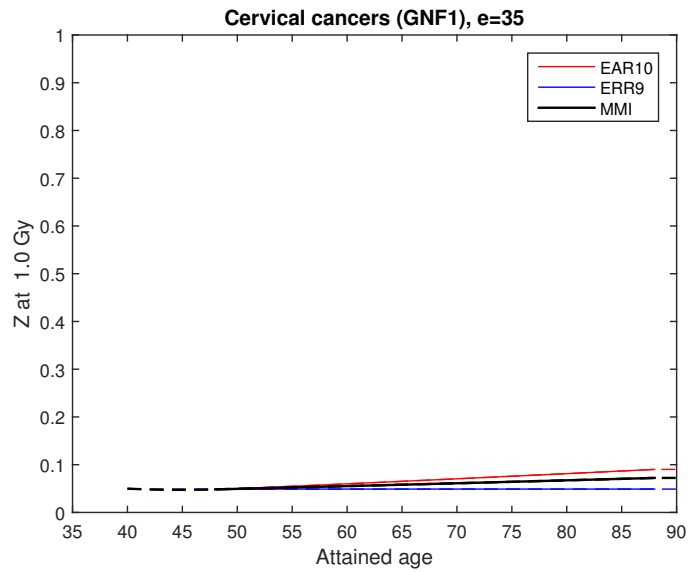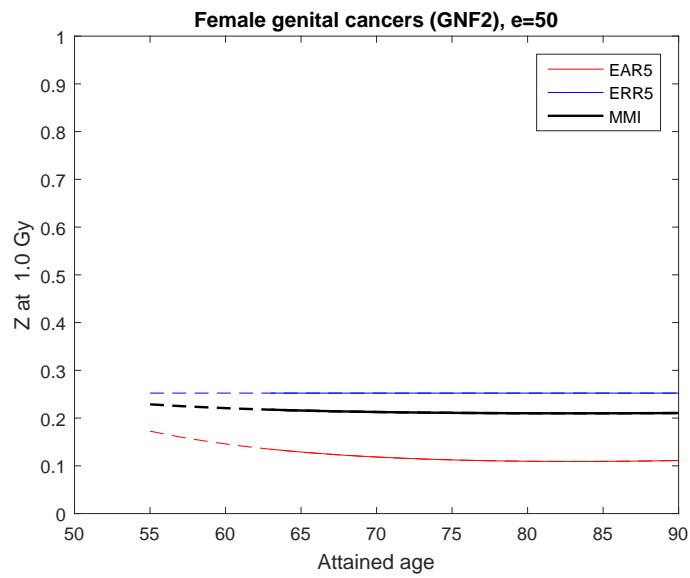
Figure 8.8: Probability of causation for female genital cancers (GNF2 group) for female exposed at age 50 using estimated partial models (blue, red) and their MMI-aggregate (black). Dashed lines indicate extrapolations beyond the LSS cohort-supported range.

9 Male genital organs (GNM group)

The group of male genital cancers includes 387 prostate cancers (ICD10:C61) and 16 cancers of other male genital organs (ICD10:C60,C63). Originally attributed to the GNM group, 17 cases of testes cancers (ICD10:C62) were re-assigned to the group of remaining cancers (REM), because of distinctively different age dependence of testes cancer incidence rate. Unlike prostate cancer, the incidence rate of testes cancer starts raising after age 15, approaches maximum values at ages 30–35, and reduces to minimal rates after age 50–55.

Due to the overwhelming number of prostate cancer cases (387 of 403), the model fitting was performed with doses for bladder. The comparison of these and weighted colon doses is shown in Fig. 9.1.

For manual preparation of input data for ProZES, the group GNM should be indicated by the code value 104.

A Poisson regression of the cancer cases belonging to the group GNM resulted in three models: two of ERR-type and one of EAR-type (see Table 9.1). Correspondingly, these models are designated here as 'GNM-EAR7', 'GNM-ERR8a', and 'GNM-ERR8b'. The terms and notations used in the model equations below are those of the generic model, which is fully described in Section 5.2.

In the selected models, the parametric baseline is described using simple representation which accounts only for effects of age and birth year. However, despite of general similarity, the baseline rate representations for different models vary. For example, the baseline equation for the 'GNM-EAR7' model includes no quadratic spline term and appears as follows:

$$\lambda_0(10^{-4}PY^{-1}) = \exp\left[\beta_1 + \beta_5 \ln\frac{a}{70} + \beta_7 \ln^2\frac{a}{70} + \beta_9\frac{b-1915}{10} + \beta_{11}\left(\frac{b-1915}{10}\right)^2\right] \tag{9.1}$$

with the risk function in the following form:

$$EAR(10^{-4}PY^{-1}) = \beta_{19}D\exp\left[\beta_{25}\ln\frac{a}{70}\right]. \tag{9.2}$$

Table 9.1: Statistical properties of the models fitted to characterize risk of cancers of male genital organs (group GNM) for members of the LSS cohort

Model type (name)	K	Estimated cases: baseline	excess	Deviance	ΔAIC	AIC-weight (%)
EAR (GNM-EAR7)	7	396.2	6.8	1518.05	5.565	4.72
ERR (GNM-ERR8a)	8	398.6	4.4	1510.48	—	76.35
ERR (GNM-ERR8b)	8	396.7	6.3	1513.27	2.789	18.93
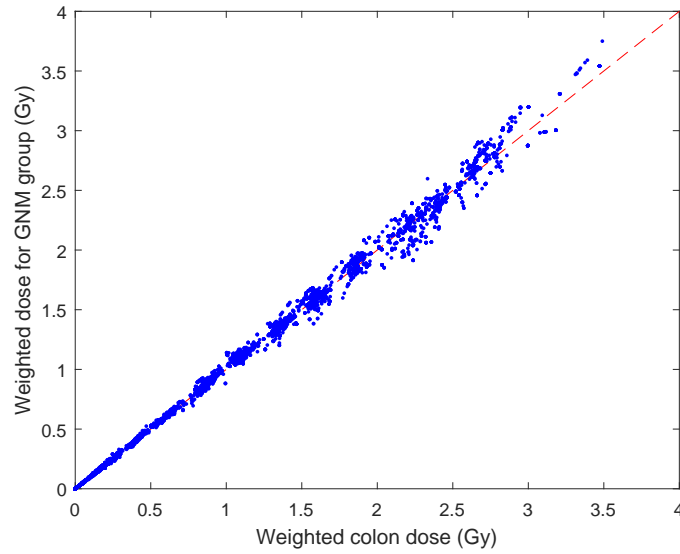
Figure 9.1: Comparison of average weighted dose for the male genital cancers (group GNM) with weighted colon dose

The model 'GNM-ERR8a' is formulated with the following baseline function:

$$\lambda_0(10^{-4} PY^{-1}) = \exp\left[\beta_1 + \beta_5 \ln\frac{a}{70} + \beta_7 \ln^2\frac{a}{70} + \right.$$
$$\left. + \beta_9 \frac{b-1915}{10} + \beta_{11}\left(\frac{b-1915}{10}\right)^2 + \beta_{13}\max^2\left(0, \ln\frac{a}{\beta_{15}}\right)\right] \tag{9.3}$$

and with a simple, constant linear-dose-response risk model:

$$ERR = \beta_{19}D. \tag{9.4}$$

The model 'GNM-ERR8b' has a simpler baseline function:

$$\lambda_0(10^{-4} PY^{-1}) = \exp\left[\beta_1 + \beta_5 \ln\frac{a}{70} + \beta_7 \ln^2\frac{a}{70} + \beta_9 \frac{b-1915}{10} + \beta_{13}\max^2\left(0, \ln\frac{a}{\beta_{15}}\right)\right] \tag{9.5}$$

with radiation risk including also an attained-age effect modifier:

$$ERR = \beta_{19}D\exp\left(\beta_{25}\ln\frac{a}{70}\right) \tag{9.6}$$

Parameter values and statistics are shown in Table 9.2. As seen from the table parameters of the radiation risk functions show low statistical significance. This fact is reflected by the large variability range of assigned share estimates (see Z-figures below). In the figures, extrapolation beyond the range supported by the LSS follow-up data is indicated by dashed lines (see details in Chapter 6).

Table 9.2: Parameters and parameter statistics for the selected models of the group GNM for cancers of male genital organs

Parameter	EAR-type model (GNM-EAR7)		ERR-type model (GNM-ERR8a)		ERR-type model (GNM-ERR8b)	
	Estimate (p-value)	95%CI	Estimate (p-value)	95%CI	Estimate (p-value)	95%CI
β_1	2.36 (<0.001)	(2.28; 2.51)	2.78 (<0.001)	(2.39; 4.7)	2.75 (<0.001)	(2.38; 4.8)
β_5	10.8 (<0.001)	(9.3; 12.3)	17.5 (<0.001)	(11.7; 25.4)	16.1 (<0.001)	(10.6; 27.6)
β_7	−13.8 (<0.001)	(−17.2; −6.9)	8.2 (0.010)	(−4.2; 9.8)	6.82 (0.087)	(−8.6; 8.8)
β_9	−0.32 (<0.001)	(−0.45; −0.19)	−0.32 (<0.001)	(−0.39; −0.2)	−0.25 (<0.001)	(−0.34; −0.15)
β_{11}	0.043 (0.078)	(−0.005; 0.09)	0.044 (0.061)	(−0.002; 0.089)	—	—
β_{13}	—	—	−24.5 (<0.001)	(−99.7; −9.98)	−21.3 (<0.001)	(−341; −6.6)
β_{15}	—	—	61.5 (<0.001)	(54.2; 110)	61.7 (<0.001)	(54; 114)
β_{19}	1.39 (0.38)	(−0.14; 5.2)	0.12 (0.56)	(−0.083; 0.62)	0.20 (0.37)	(−0.016; 0.74)
β_{25}	2.7 (0.27)	(−7.0; 42.6)	—	—	−3.7 (0.33)	(−7.4; 26.7)
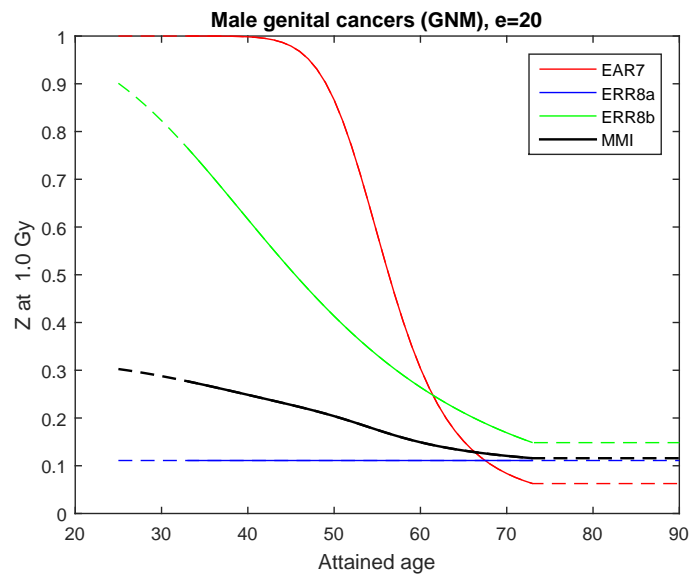
Figure 9.2: Probability of causation for the ProZES risk models for male genital cancers (GNM group) for age at exposure 20. Shown are partial models (coloured lines) and their MMI aggregate (black). Dashed lines indicate extrapolations beyond the LSS cohort-supported range.
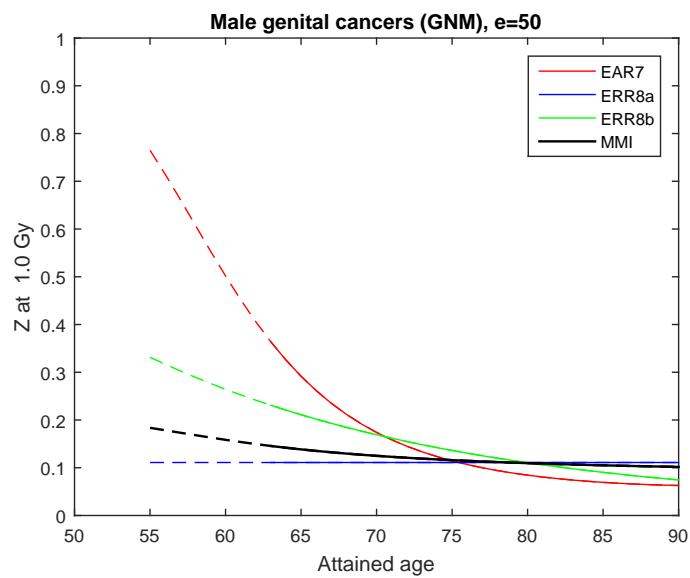
Figure 9.3: Probability of causation for the ProZES risk models for male genital cancers (GNM group) for age at exposure 50. Shown are partial models (coloured lines) and their MMI aggregate (black). Dashed lines indicate extrapolations beyond the LSS cohort-supported range.

10 Cancers of brain and central nervous system (BCNS group)

The number of cases of brain and central nervous system (CNS) cancers in the LSS cohort (LSS code: 'cnsca') is not high: 281 cases, therefore one would not expect sophisticated models to be developed and justified for this group.

In the LSS cohort, the group of brain and central nervous system cancers includes malignant and benign tumours as well as tumours of uncertain behaviour, i.e. diseases indicated according to the ICD10 classification by codes C70–C72, D32. According to Preston et al. (2007), benign neoplasms are mostly represented by meningioma (ICD10:D32) and schwannoma (ICD10:C72.4).

Weighted (neutron and gamma) doses to brain from the LSS dataset have been used to fit the radiation effect. In average, these doses are systematically higher (approx. 10%) than the weighted colon doses (see Fig. 10.1), spanning a range up to 4.5 Gy.

For manual preparation of input data, diagnoses of the group BCNS should be specified using a ProZES-specific internal code value 106.

The risk model of Preston et al. (2007) for brain and CNS cancers suggests constant risk, either ERR or EAR, without any effect modifiers. Their model results in deviance 1853.94 and encounters 16 parameters, many of them appear statistically non-significant.

For the purposes of the present study, the LSS data for brains and CNS cancers have been fitted using the generic model structure (5.2)–(5.6) as was used for other grouped cancers (DIG, URI, REM, etc) and described in the Section 5.2. If only statistically significant parameters, which comply with likelihood ratio test and the AIC-criterion, are kept, then the fit ends up with two winning models of EAR- and ERR-type. Main statistical properties of these models are shown in Table 10.1. The terms and notations used in the model equations below are those of the generic model, which is fully described in Section 5.2.

The fitted models have the following common parametric form for the function describing baseline

Table 10.1: Statistical properties of the models fitted to characterize risk of cancers of brain and central nervous system (group BCNS) for members of the LSS cohort

| Model type (name) | K | Estimated cases [a] | | Deviance | ΔAIC | AIC-weight (%) |
		baseline	excess			
EAR (BCNS-EAR6)	6	236.9	10.2	1870.31	0.65	41.91
ERR (BCNS-ERR7)	7	233.9	12.1	1867.66	—	58.09

[a] Screening effect of the autopsy program (mostly, before 1970) is excluded
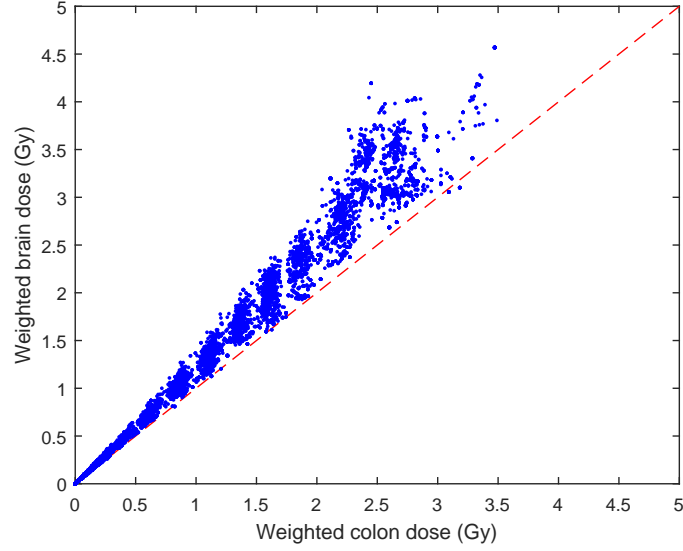
Figure 10.1: Comparison of average weighted dose for the group of brain and central nervous system cancers (BCNS group) with weighted colon dose

rate:

$$\lambda_0(10^{-4}\,PY^{-1}) = \exp\left[\beta_1 + \beta_4 IC + \beta_5 \ln\frac{a}{70} + \beta_9 \frac{b-1915}{10}\right], \tag{10.1}$$

and radiation risk is specified using constant linear-dose-response EAR-type model:

$$EAR(10^{-4}\,PY^{-1}) = \beta_{19}D, \tag{10.2}$$

and linear-dose-response ERR-type model with attained-age effect modifier:

$$ERR = \beta_{19}D\exp\left[\beta_{25}\ln\frac{a}{70}\right]. \tag{10.3}$$

For cancers of the BCNS group, screening factor for the LSS cohort

$$F_{scr} = \exp\left(\beta_{33}\mathrm{sign}\,(cy-1970)\right). \tag{10.4}$$

has been found highly significant ($p = 0.007$, see Table 10.2). Correspondingly, for target populations other than the LSS cohort the screening factor related to condition of minimum or no screening, i.e. for time after 1970, has been selected for implementation in ProZES: $F_{scr} = \exp(\beta_{33})$.

The parameters values and their statistics are shown in the following Table 10.2. As seen from the table, the models do not contain quadratic terms for calendar year (age at exposure) effect. Such terms are present in the models of Preston et al. (2007) and have been found statistically significant in the present fits with a deviance change of approximately 10–15, depending on the model. However,

Table 10.2: Parameters and their statistics for the BCNS cancer group risk models

Parameter	ERR-type model (BCNS-ERR7)			EAR-type model (BCNS-EAR6)		
	Estimate	(p-value)	95%CI	Estimate	(p-value)	95%CI
β_1	0.26	(0.16)	$(-0.10; 0.61)$	0.23	(0.21)	$(-0.13; 0.57)$
β_4	0.63	(<0.001)	$(0.46; 0.99)$	0.64	(<0.001)	$(0.47; 0.99)$
β_5	3.91	(<0.001)	$(3.42; 4.92)$	3.77	(<0.001)	$(3.28; 4.76)$
β_9	-0.36	(<0.001)	$(-0.52; -0.19)$	-0.34	(<0.001)	$(-0.51; -0.17)$
β_{19}	0.24	(0.23)	$(0.045; 0.79)$	0.46	(0.046)	$(0.24; 0.99)$
β_{25}	-2.97	(0.009)	$(-5.2; -0.66)$	—	—	—
β_{33}	-0.31	(0.007)	$(-0.53; -0.086)$	-0.27	(0.015)	$(-0.49; -0.06)$

these models lead to unrealistic shapes of baseline incidence, especially when extrapolated beyond the considered follow-up period (i.e. after 1998). This fact and the relatively small number of cancer cases in the BCNS group (281 cases) justified rejection of the models with quadratic calendar year effects, thus leading to acceptance of less sophisticated albeit robust models with linear effects in baseline exponential term. As seen from the above shown Eqns. (10.1)–(10.4) and from Table 10.2, both models are sex-independent, because no significant gender effect was found.
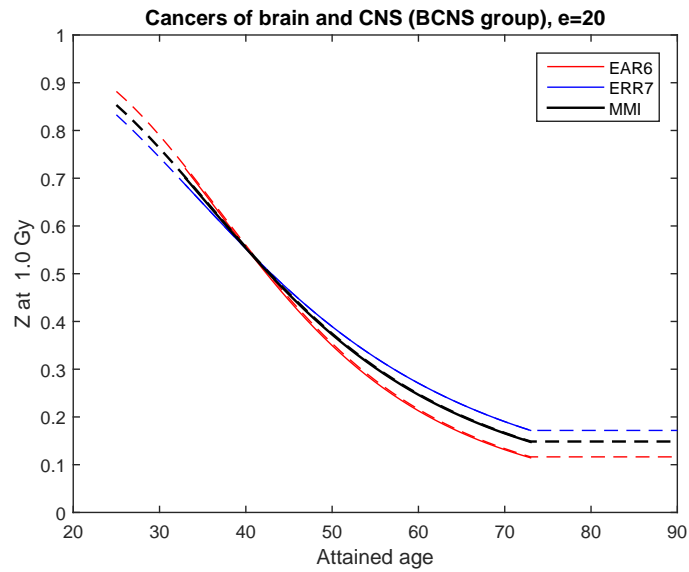
Figure 10.2: Probability of causation Z for the ProZES risk models for cancers of the BCNS group for age at exposure 20. Shown are partial models (red and blue) and their MMI-aggregate (black). Dashed lines indicate extrapolation beyond the LSS cohort-supported range.
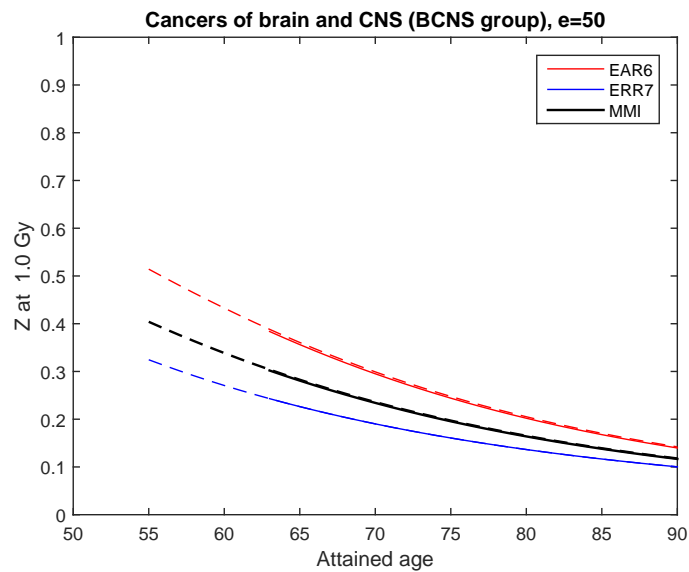
Figure 10.3: Probability of causation Z for the ProZES risk models for cancers of the BCNS group for age at exposure 50. Shown are partial models (red and blue) and their MMI-aggregate (black). Dashed lines indicate extrapolation beyond the LSS cohort-supported range.

11 Non-melanoma skin cancer (group SKIN)

In the LSS cohort, doses (Young and Kerr, 2005) for skin are generally higher than that for colon or other internal organs. The weighted skin doses are compared to weighted colon doses in Fig. 11.1.

The non-melanoma cancers in the LSS cohort include malignancies of basal and squamous cells. The LSS data might suggest radiation-attributable cases only for basal cell cancers, and no radiation effect for squamous cell carcinomas (Kaiser and Walsh, 2015). This observation seems to be supported by observations of effects of UV-radiation on development of skin cancers (Kraemer et al., 2013). However, in the analysed LSS dataset, which encompass follow-up period from 1958 to 1998, the total number of non-melanoma skin cancers (330 cases) and attributable fraction (crude estimate is $\approx$23%, see Preston et al. 2007) are not high thus not justifying further separation of the data according to skin cancer types. It is anticipated that the new LSS data for the extended follow-up period will include significantly larger number of the skin malignancies, because of the cohort ageing. Therefore, in the present analysis the whole group of non-melanoma skin cancers is analysed, without further sub-division.

Crude estimates of relative risk show very low or no radiation-attributable skin cancer cases for doses less than 1 Gy, thus suggesting a strong non-linear dose response. Correspondingly, during fitting the risk models for skin cancers linear, quadratic, power and exponential shapes for dose response have been tried and the power form has been found as statistically significant and leading to a family of the best descriptive models. The summary of statistical properties of the selected models, including their AIC-based weights used for MMI aggregation, is shown in Table 11.1. As seen from the table, the selected models includes one model of ERR-type ('SKIN-ERR8') and one model of EAR-type ('SKIN-EAR10'). The model selection has been based on parsimonious parameter choice, i.e. the model parameters have been considered as significant if passed both AIC- and likelihood ratio tests. The terms and notations used in the model equations below are those of the generic model, which is fully described in Section 5.2.

For the purposes of input data preparation, non-melanoma skin cancers (group SKIN) are coded using internal ProZES-specific code 107.

The fitted risk models share the same form of parametric baseline:

$$\lambda_0(10^{-4}PY^{-1}) = \exp\ \beta_1 + \beta_2 s + \beta_4 IC + (\beta_5 + \beta_6 s)\ln\frac{a}{70} + \beta_7\ln^2\frac{a}{70} \qquad (11.1)$$

with the only exception that in the ERR-type model the age- and gender-dependent term (β_6 in the above equation) was rejected by likelihood-ratio test albeit satisfying AIC selection criterion.

The functions used to describe radiation risk for cancers of the group SKIN demonstrate non-linear dose response, characterised by power of approximately 3/2. Besides dose response, the risk
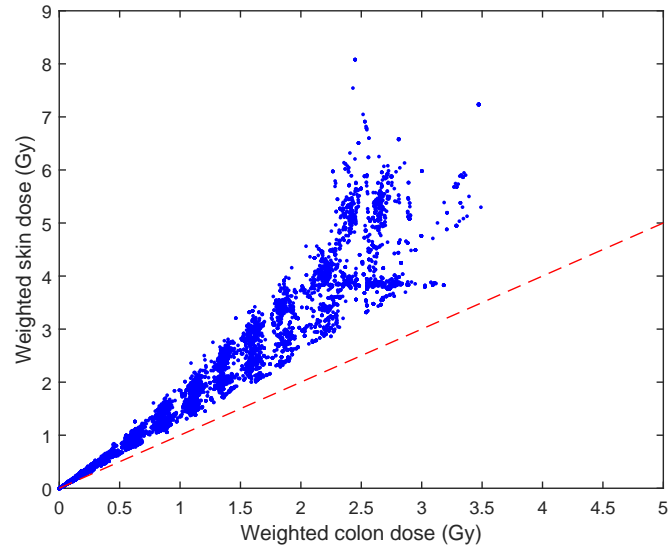
Figure 11.1: Comparison of average weighted dose for the group of non-melanoma skin cancers (SKIN group) with weighted colon dose

Table 11.1: Statistical properties of the models fitted to characterize risk of non-melanoma skin cancers (group SKIN) for members of the LSS cohort

| Model type (name) | K | Estimated cases | | Deviance | ΔAIC | AIC-weight (%) |
		baseline	excess			
ERR (SKIN-ERR8)	8	291.4	38.6	2061.85	—	71.71
EAR (SKIN-EAR10)	10	293.1	36.9	2059.71	1.86	28.29

Table 11.2: Maximum likelihood estimates (MLE) and statistics of parameters for the selected models of radiation risk for non-melanoma skin cancers (group SKIN)

Parameter	ERR-type model (SKIN-ERR8)			EAR-type model (SKIN-EAR10)		
	Estimate	(p-value)	95%CI	Estimate	(p-value)	95%CI
β_1	0.30	(0.028)	(0.03; 0.56)	0.31	(0.027)	(0.04; 0.57)
β_2	−0.12	(0.029)	(−0.18; −0.01)	−0.16	(0.015)	(−0.22; −0.03)
β_4	0.35	(0.022)	(0.20; 0.65)	0.35	(0.020)	(0.20; 0.66)
β_5	6.53	(<0.001)	(6.2; 7.2)	6.33	(<0.001)	(5.6; 7.1)
β_6	—	—	—	0.91	(0.010)	(0.57; 1.6)
β_7	3.05	(<0.001)	(2.1; 3.9)	2.36	(0.001)	(0.9; 3.7)
β_{19}	0.71	(0.018)	(0.42; 1.46)	1.12	(0.021)	(0.65; 2.3)
β_{21}	1.55	(<0.001)	(1.3; 2.1)	1.60	(<0.001)	(1.3; 2.2)
β_{25}	—	—	—	3.65	(<0.001)	(2.7; 5.9)
β_{29}	−0.89	(<0.001)	(−1.26; −0.56)	−0.75	(<0.001)	(−1.2; −0.35)

function for the ERR-type model has only age-at-exposure modifier:

$$ERR = \beta_{19} D^{\beta_{21}} \exp\left(\beta_{29}\frac{e-30}{10}\right), \tag{11.2}$$

while risk function of the EAR-type model includes also parameter dependent on attained age:

$$EAR\left(10^{-4}PY^{-1}\right) = \beta_{19} D^{\beta_{21}} \exp\left(\beta_{25}\ln\frac{a}{70} + \beta_{29}\frac{e-30}{10}\right). \tag{11.3}$$

Parameters of the models selected for the SKIN model group are shown in Table 11.2.

The non-linear power dose response of the above described models may result in lower values of radiation risk and assigned share following fractionated exposures, than the values of risk and assigned share estimated for a single exposure with the same dose. Currently available epidemiological data for the LSS cohort do not suggest alternative shapes of the dose responses due to no evidence of radiation risk at dose less than 1 Gy. Correspondingly, the models with non-linear dose response shown above have been implemented in ProZES and can be suggested for use until new epidemiological or other data will allow to justify alternative shape(s) of the dose response. Presently, in case of fractionated low-dose exposures it could be advised to calculate additionally, as a conservative upper limit, a value of assigned share using the single exposure with dose equal to the total dose due to the fractionated exposures.

Figure 11.2: Probability of causation Z for the ProZES risk models for cancers of the SKIN group for a male exposed at age 20. Shown are partial models (red and blue) and their MMI-aggregate (black). Dashed lines indicate extrapolation beyond the LSS cohort-supported range.

Figure 11.3: Probability of causation Z for the ProZES risk models for cancers of the SKIN group for a female exposed at age 20. Shown are partial models (red and blue) and their MMI-aggregate (black). Dashed lines indicate extrapolation beyond the LSS cohort-supported range.

Figure 11.4: Probability of causation Z for the ProZES risk models for cancers of the SKIN group for a male exposed at age 50. Shown are partial models (red and blue) and their MMI-aggregate (black). Dashed lines indicate extrapolation beyond the LSS cohort-supported range.
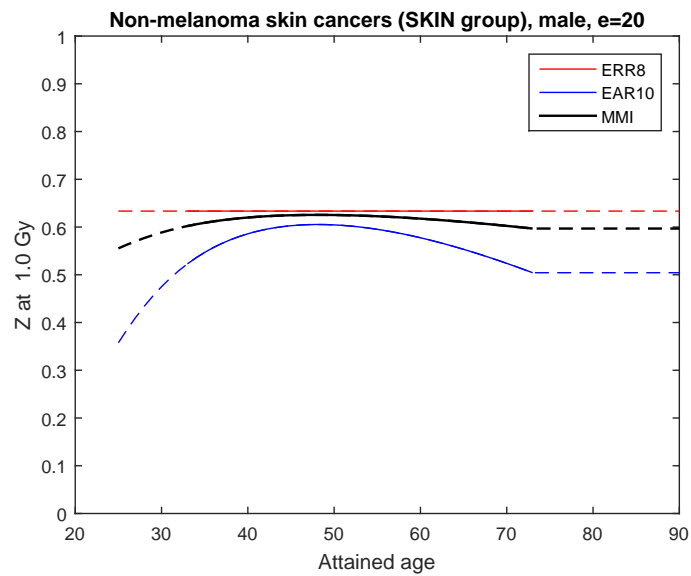
Figure 11.5: Probability of causation Z for the ProZES risk models for cancers of the SKIN group for a female exposed at age 50. Shown are partial models (red and blue) and their MMI-aggregate (black). Dashed lines indicate extrapolation beyond the LSS cohort-supported range.
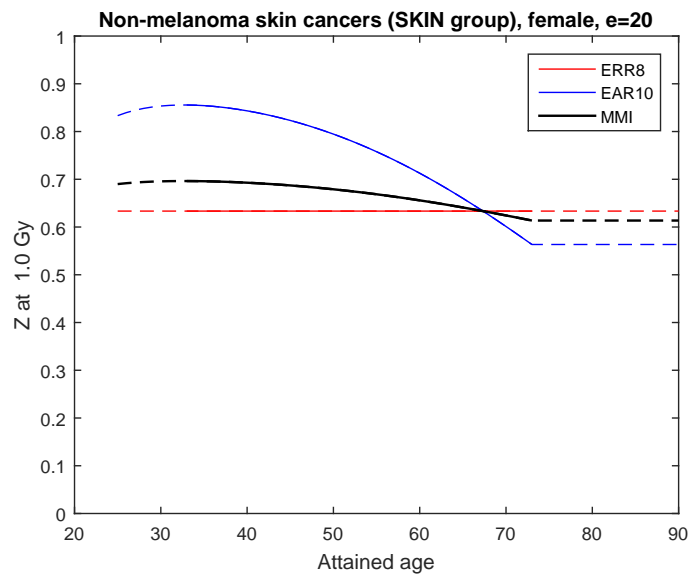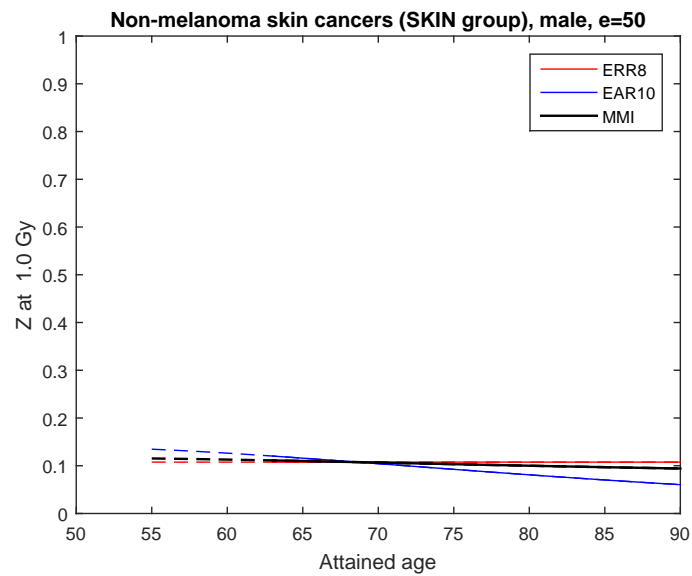
12 Solid cancers of the remaining organs (REM group)

The cancer group REM is formed from solid cancers of the remaining, i.e. not modelled explicitly or as a part of functionally-grouped, cancers. This group includes cancers of: nasal cavity, middle ear and assessor sinuses (ICD10:C30, C31), larynx (ICD10:C32), other parts of respiratory system (ICD10:C37–39), thymus (ICD10:C37), bone (ICD10:C40,C41), connective tissue (ICD10:C47,C49), and testes (ICD10:C62). In a total, this group combines 324 solid cancer cases (see Table 5.1).

Among cancers observed in the LSS cohort during the period 1958–1998 (Preston et al. 2007), there are 254 'other solid' cancer cases, marked as 'othsol' in the LSS database. This group combines together cancers of eyes and endocrine glands (excluding thyroid), secondary cancers of lymph nodes, and other, ill- or non-specified cancers. Comparison of incidence rates suggests that most of the cancers cases in this group come from secondary or non-specified diseases. Due to this, inclusion of these cases into the REM group is not justified and, consequently, these cases have not been included in the REM group.

Testes were attributed to the REM group, because of age-dependence of baseline incidence rate appeared incompatible to other cancers of male genital system, of which prostate cancers are most frequent.

Weighted dose for fitting cancer risk models for the REM group has been obtained as weighted by the number of cases average doses for several organs, which can serve as mock for the organs in the REM group. Namely, brain dose for cancers of nasal region, thyroid dose for larynx, lung dose for other respiratory organs, liver dose for thymus, and skeleton dose for bone and connective tissues. The average weighted dose for the REM group, as seen from Fig. 12.1, is approximately 20% higher than corresponding colon weighted dose.

For the purposes of input data preparation, diagnoses of diseases belonging to the group REM are indicated by internal ProZES-specific code 102.

Fitting of the cancer cases belonging to the REM group ended up with two models of EAR- and ERR-types. Statistical properties of the models, including their AIC-based weights, are shown in Table 12.1. The terms and notations used in the model equations below are those of the generic model, which is fully described in Section 5.2.

Baseline shape is the same for the both risk models and appears as follows:

$$\lambda_0 = \exp \left[\beta_1 + \beta_2 s + \beta_4 IC + \beta_5 \ln \frac{a}{70} + \beta_7 \ln^2 \frac{a}{70} + \right.$$

$$\left. + \beta_9 \frac{by - 1915}{10} + (\beta_{13} + \beta_{14} s) \max^2 \left[0, \ln \frac{a}{\beta_{15}} \right] \right]$$

(12.1)
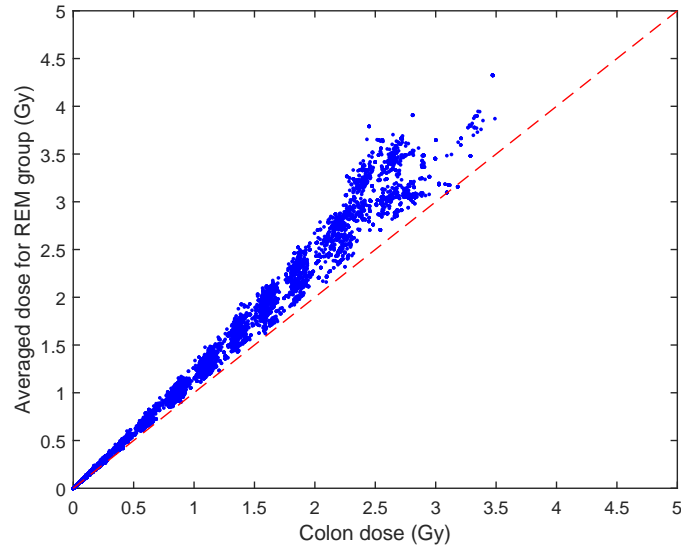
Figure 12.1: Averaged weighted dose for organs of the REM group compared to weighted colon dose as given in the LSS cancer incidence database for the follow-up period 1958–1998

Table 12.1: Statistical properties of the models fitted to characterize risk of cancer for remaining organs (group REM) for members of the LSS cohort

Model type (name)	K	Estimated cases		Deviance	ΔAIC	AIC-weight (%)
		baseline	excess			
ERR (REM-ERR11)	11	308.6	15.4	2031.12	—	67.04
EAR (REM-EAR11)	11	309.6	14.4	2032.54	1.42	32.96

Table 12.2: Parameters and their statistics for the fitted risk models of solid cancers of remaining organs (group REM) among members of the LSS cohort

Parameter	ERR-type model (REM-ERR11)			EAR-type model (REM-EAR11)		
	Estimate	(p-value)	95%CI	Estimate	(p-value)	95%CI
β_1	0.95	(0.007)	(0.27; 2.72)	0.90	(0.037)	(0.48; 4.3)
β_2	−0.57	(<0.001)	(−0.65; −0.41)	−0.56	(<0.001)	(−0.64; −0.37)
β_4	0.41	(0.006)	(0.26; 0.71)	0.41	(0.005)	(0.27; 0.7)
β_5	5.32	(<0.001)	(2.6; 10.3)	5.01	(0.005)	(1.5; 8.6)
β_7	2.03	(0.084)	(−2.5; 4.4)	1.76	(0.25)	(−1.2; 4.8)
β_9	0.12	(0.018)	(0.07; 0.21)	0.12	(0.016)	(0.07; 0.22)
β_{13}	−9.83	(0.001)	(−197; −4.4)	−9.57	(0.005)	(−36; −3.4)
β_{14}	−2.34	(0.12)	(−26; −0.19)	−2.56	(0.18)	(−17.5; 0.23)
β_{15}	55.5	(<0.001)	(46.4; 85.2)	55.9	(<0.001)	(32; 100)
β_{19}	0.25	(0.20)	(0.06; 0.76)	0.60	(0.030)	(0.33; 1.24)
β_{20}	—	—	—	-0.41	(0.136)	(−0.95; 0.048)
β_{25}	−2.77	(0.019)	(−5.1; −0.43)	—	—	—

Radiation risk in the ERR-type model is expressed with age-dependent modifier:

$$ERR = \beta_{19} D \exp\left(\beta_{25} \ln \frac{a}{70}\right), \tag{12.2}$$

while in the EAR-type model no statistically significant effect modifiers have been found:

$$EAR(10^{-4}PY^{-1}) = (\beta_{19} + \beta_{20}s) D. \tag{12.3}$$

The complete set of the model parameter values for risk and baseline functions can be found Table 12.2. In ProZES, the both model are aggregated, using their AIC weights, into the MMI-combined model. Correspondingly, assigned shares derived from the partial models and from their MMI-based compound are shown in Figs. 12.2–12.5. In the figures, extrapolation beyond the range supported by the LSS follow-up data is indicated by dashed lines (see details in Chapter 6).

Figure 12.2: Probability of causation Z for the ProZES risk models for cancers of the REM group for a male exposed at age 20. Shown are partial models (red and blue) and their MMI-aggregate (black). Dashed lines indicate extrapolation beyond the LSS cohort-supported range.

Figure 12.3: Probability of causation Z for the ProZES risk models for cancers of the REM group for a female exposed at age 20. Shown are partial models (red and blue) and their MMI-aggregate (black). Dashed lines indicate extrapolation beyond the LSS cohort-supported range.

Figure 12.4: Probability of causation Z for the ProZES risk models for cancers of the REM group for a male exposed at age 50. Shown are partial models (red and blue) and their MMI-aggregate (black). Dashed lines indicate extrapolation beyond the LSS cohort-supported range.
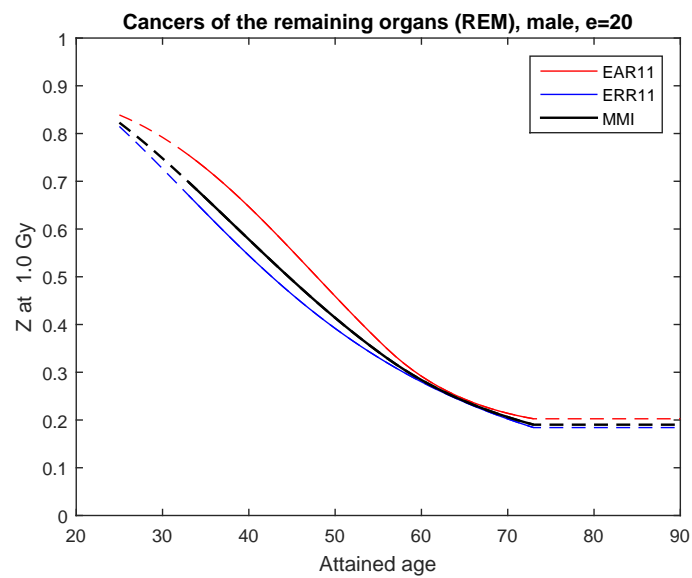
Figure 12.5: Probability of causation Z for the ProZES risk models for cancers of the REM group for a female exposed at age 50. Shown are partial models (red and blue) and their MMI-aggregate (black). Dashed lines indicate extrapolation beyond the LSS cohort-supported range.
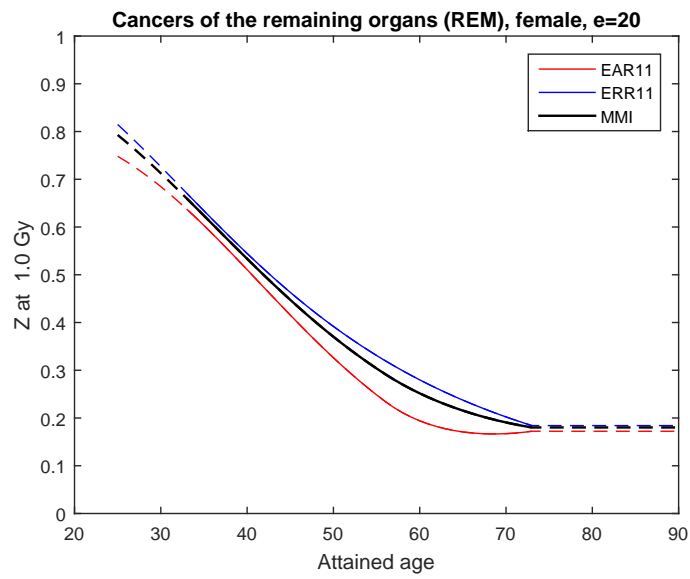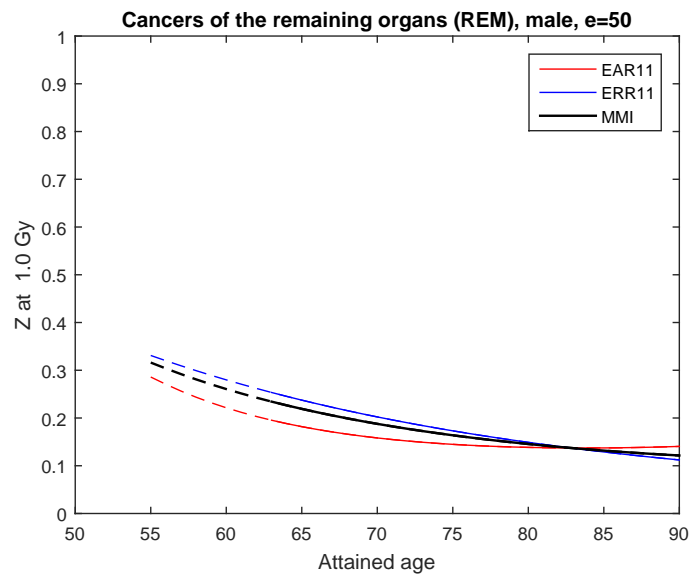
13 Cancers of hematopoietic system

The models for radiation risk of leukaemia had been derived from the LSS cohort incidence data collected for more than 50 years, in the period from 1950 to 2001 (Hsu et al., 2013). The present analysis uses the same grouping of leukaemia sub-types, as suggested by Hsu et al. (2013), so, not surprisingly, that some leukaemia models fitted in the present study appear very similar to the results obtained in the preceding study. There were at least two reasons of not using the results reported by Hsu et al. (2013) and of complete re-fitting the leukaemia data. First, stochastic sampling of radiation risk requires using not only the best estimates of model parameters but also their full covariance matrices, including parametric baseline rates. Second, the multi-model inference methodology adopted in ProZES assumes that not only the 'preferable' model which provides the best statistical quality should be used for risk estimation but a family of the models with comparably similar statistical significance should be applied for the risk simulations. Neither of these was available in the paper of Hsu et al. (2013), thus justifying new independent analysis using descriptive models.

Totally 944 leukaemia cases in the 1950–2001 follow-up data had been reported by (Hsu et al., 2013) as legitimate for radiation risk quantification and fitting. Of this number, there were:

- 43 cases of acute lymphoblastic leukaemia (ALL);

- 449 cases of chronic lymphocytic leukaemia (CLL) and lymphomas of Hodgkin and non-Hodgkin types;

- 176 cases of acute and other myeloid leukaemia (AML);

- 75 cases of chronic myeloid leukemia (CML);

- 136 cases of multiple myeloma (MM);

- 47 cases of adult T-cell leukaemia; and

- 18 cases of other leukaemia types.

Adult T-cell leukaemia is known to be caused by infection of viral origin (Takatsuki, 2005), thus it was excluded from the radiation risk modelling. The 18 cases of other leukaemia types were also excluded from the analysis as this number is insufficient for radiation risk modelling. The rest cases have been grouped into five groups indicated as L1, L2, ..., L5, accordingly. Descriptive models of radiation risk with various types of dose response, including linear, quadratic, exponential, spline, threshold dose response forms and their combinations, have been fitted to model the grouped incidence data. For the purposes of manual preparation of input data, the leukaemia groups are indicated using the following internal codes: 201 for the group L1 (ALL), 202 for the group L2

(CLL, HL, nHL), 203 for the group L3 (AML), and 204 for the group L4 (CML). See also Table 5.3 for ICD10 codes of diseases in the specific groups.

Incidence data for the group L5 (multiple myeloma, MM) had shown no dose effect, thus no radiation risk model(s) were developed for this group. For the remaining four groups, the fitting resulted in a series of models, which have created a framework for MMI-based modelling of leukaemia radiation risks and are described in details below. The fitting was performed using doses for red bone marrow.

Unlike generic models for solid cancers (see Section 5.2), the descriptive models for leukaemia use different indicator variables for sex, city of residence, and presence in the city at the time of bombing:

$$
m = \begin{matrix} 1 & \text{male} \\ 0 & \text{female} \end{matrix} \qquad f = \begin{matrix} 0 & \text{male} \\ 1 & \text{female} \end{matrix} \qquad n = \begin{matrix} 0 & \text{Hiroshima} \\ 1 & \text{Nagasaki} \end{matrix} \qquad (13.1)
$$

$$
NIC_{Hi|Na} = \begin{matrix} 0 & \text{in city (Hi – Hiroshima, Na – Nagasaki)} \\ 1 & \text{not-in-city (Hi – Hiroshima, Na – Nagasaki)} \end{matrix} \qquad (13.2)
$$

Radiation risk of hematopoietic malignancies is known to demonstrate complex dose responses (UNSCEAR, 2009; BEIR, 2006), which are often best represented by non-linear shapes, e.g. quadratic, exponential curves or various spline shapes. The risk estimates usually come from the higher dose range, say around 1 Gy and above. Correspondingly, parameters of dose responses are defined there and the risk estimates derived using various shapes of dose response comply to each other in this dose range. However, extrapolation of the estimated risk functions to lower dose range, say below 0.1 Gy, may result in highly divergent behaviour of the non-linear risk functions in comparison to pure linear dose responses. For example, linear and quadratic dose responses, which otherwise result in the same risk value at dose 1 Gy, will differ 10 times at dose 0.1 Gy and 100 times at dose 10 mGy. Such behaviour would result in strong reduction of radiation risk estimates based on quadratic response for fractionated exposures. Because the available epidemiological data do not allow to unambiguously justify a selection of either type of the dose response, so choosing a risk estimate coming from the linear response appears as a reasonably conservative solution.

Practical implementation in ProZES of this conservative model selection uses so-called 'twins', i.e. models of the same type, sharing the same equations to characterise baseline rate and risk, differing only by type of the dose response shape. If within the course of MMI-based model sampling any of the non-linear twin model has been selected, then the alternative linear twin model is used to evaluate risk estimates, as well. Then, the maximum risk estimate of the two is selected and used in calculation of assigned share. This procedure is applied for the risk models derived for the groups L1, L3, and L4 (see details below).

13.1 Leukaemia group L1 (ALL)

For the group L1 (code 201), the fitting ended up with only two applicable models:

- EAR-LNT model of EAR-type with linear non-threshold (LNT) dose response ($w_{AIC} = 90.18\%$);

Table 13.1: Parameters (MLE and standard deviations) of the fitted models for radiation and baseline risks of the group L1 leukaemias

Parameter	EAR-LNT		EAR-QDR	
	MLE	σ	MLE	σ
β_1	-2.334	0.295	-2.297	0.283
β_2	1.700	0.766	1.267	0.814
β_3	-0.020	0.567	-0.137	0.557
β_4	-0.134	1.036	-0.274	1.032
β_5	-1.810	0.372	-1.869	0.384
β_6	-0.922	0.480	-0.908	0.514
β_7	0.232	0.121	0.174	0.093

- EAR-QDR model of EAR-type with pure quadratic (QDR) dose response ($w_{AIC} = 9.82\%$).

The models share the same form of the parametric baseline:

$$\lambda_0(10^{-4}PY^{-1}) = \exp\left[\beta_1 + \beta_2 \ln\frac{a}{70} + \beta_3 NIC_{Hi} + \beta_4 NIC_{Na}\right]. \tag{13.3}$$

The risk functions have different dose response but the same effect modifiers. Namely, for the model with linear dose response:

$$EAR_{LNT}(10^{-4}PY^{-1}) = \beta_7 D \exp\left[\beta_5 \ln\frac{a}{70} + \beta_6 f\right] \tag{13.4}$$

and for the model with quadratic response:

$$EAR_{QDR}(10^{-4}PY^{-1}) = 1.12\beta_7 D^2 \exp\left[\beta_5 \ln\frac{a}{70} + \beta_6 f\right]. \tag{13.5}$$

The model parameters and their standard deviations age shown in the following Table 13.1

As seen from Eqs. (13.3)–(13.5), the both selected models have the same form, differing only in shape of the dose response. That is, the both models are considered in ProZES as twins, thus they are always evaluated during simulation runs. Correspondingly, the higher value of the two radiation risk estimates is used to calculate assigned share.

13.2 Leukaemia group L2 (CLL and lymphomas)

The group L2 (internal code for input data preparation – 202) encountered relatively large number of cancer cases – 449, including 103 'not-in-city' cases. However, fitting separately male and female cases resulted in no radiation risk for females and in reasonably well defined radiation risk function for males. Fitting the both genders together also resulted in non-zero risk functions. As a result of

Table 13.2: Parameters (MLE and standard deviations) of the model selected to describe radiation risk of chronic lymphoblastic leukaemia and lymphomas (group L2)

Parameter	EAR-LNT		EAR-LNT-male		ERR-LNT		ERR-LNT-male	
	MLE	σ	MLE	σ	MLE	σ	MLE	σ
β_1	1.430	0.094	1.409	0.096	1.392	0.097	1.361	0.101
β_2	0.890	0.079	0.896	0.079	0.863	0.082	0.890	0.078
β_3	4.391	0.297	4.378	0.298	4.369	0.290	4.369	0.290
β_4	1.188	0.368	1.028	0.426	1.310	0.305	1.309	0.305
β_5	0.239	0.039	0.237	0.039	0.236	0.039	0.237	0.039
β_6	−0.058	0.020	−0.057	0.020	−0.056	0.020	−0.055	0.020
β_7	−0.086	0.124	−0.077	0.124	−0.065	0.126	−0.066	0.125
β_8	−0.176	0.226	−0.163	0.226	−0.155	0.227	−0.152	0.226
β_9	0.175	0.161	0.699	0.390	0.306	0.223	0.610	0.369

such situation, a decision was made to use for both genders an aggregated model, where the MMI-based models defined for males and for both genders are equally represented. Technically, it means that each model group, either for males or for both genders, contributes 50% to the generated sample. Within the groups, the EAR- and ERR-type models are aggregated according to their AIC-weights. Correspondingly, radiation risk for the diseases of the group L2 is characterised by a set of four linear (LNT) models:

- EAR-LNT model of EAR-type ($w_{AIC} = 21.00\%$);

- EAR-LNT-male model of EAR-type ($w_{AIC} = 35.87\%$);

- ERR-LNT model of ERR-type ($w_{AIC} = 29.00\%$); and

- ERR-LNT-male model of ERR-type ($w_{AIC} = 14.13\%$).

All selected models share the same form of the parametric baseline:

$$\lambda_0(10^{-4}PY^{-1}) = \exp\left[\beta_1 m + \beta_2 f + \beta_3 \ln\frac{a}{70} + \beta_4 m\ln^2\frac{a}{70} + \beta_5\frac{b-1915}{10} + \right.$$
$$\left. + \beta_6\left(\frac{b-1915}{10}\right)^2 + \beta_7 NIC_{Hi} + \beta_8 NIC_{Na}\right].$$

$$(13.6)$$

The risk functions for all models are of the simplest form:

$$EAR(10^{-4}PY^{-1}) = \beta_9 D \quad \text{and} \quad ERR = \beta_9 D. \tag{13.7}$$

All four models for the group L2 have linear non-threshold dose response, so, for the current model selection, there is no need to consider 'twin' models.

13.3 Leukaemia group L3 (AML)

The group L3 (code 203) combines 176 cases of acute myeloid leukaemia and related diseases (ICD10:C92.0, C92.2–C92.5, C93–C96), including 28 people who were not in the cities at the time of bombing.

The fitting resulted in four models of EAR- and ERR-types with quadratic (QDR) and threshold linear spline (TLS) dose dependencies. The models are:

- ERR-TLS model of ERR-type and threshold linear spline dose response ($w_{AIC} = 6.33\%$);

- ERR-QDR model of ERR-type and quadratic dose response ($w_{AIC} = 30.35\%$);

- EAR-TLS model of EAR-type and threshold linear spline dose response ($w_{AIC} = 8.44\%$);

- EAR-QDR model of EAR-type and quadratic dose response ($w_{AIC} = 54.87\%$).

The both models of ERR-type have the same structure of the parametric baseline rate:

$$\lambda_0(10^{-4}PY^{-1}) = \exp\left[\beta_1 m + \beta_2 f + \beta_3 \ln\frac{a}{70} + \beta_4 \ln^2\frac{a}{70} + \right.$$
$$\left. + \beta_5 \frac{b-1915}{10} + \beta_6 \left(\frac{b-1915}{10}\right)^2 + \beta_7 NIC_{Hi} + \beta_8 NIC_{Na} \right] \tag{13.8}$$

and their risk functions appear as follows with linear spline dose response:

$$ERR_{TLS} = \exp\left[\beta_9 \frac{e-30}{10} + \beta_{10} \left(\frac{e-30}{10}\right)^2 + \beta_{11} f \right] \times$$
$$\times \begin{cases} \beta_{13}D & \text{if } D < \beta_{12} \\ \beta_{12}\beta_{13} + \beta_{14}(D-\beta_{12}) & \text{otherwise} \end{cases} \tag{13.9}$$

and with pure quadratic response:

$$ERR_{QDR} = \exp\left[\beta_9 \frac{e-30}{10} + \beta_{10} \left(\frac{e-30}{10}\right)^2 + \beta_{11} f \right] \times 1.12 D^2 \beta_{12}. \tag{13.10}$$

The other two models of EAR-type also share the parametric form of the baseline rate:

$$\lambda_0(10^{-4}PY^{-1}) = \exp\left[\beta_1 m + \beta_2 f + (\beta_3 m + \beta_4 f)\ln\frac{a}{70} + (\beta_5 m + \beta_6 f)\ln^2\frac{a}{70} + \right.$$
$$\left. + \beta_7 \frac{b-1915}{10} + \beta_8 \left(\frac{b-1915}{10}\right)^2 + \beta_9 NIC_{Hi} + \beta_{10} NIC_{Na} \right] \tag{13.11}$$

Table 13.3: Maximum likelihood estimates and standard deviations of the model parameters selected to describe radiation risk of acute myeloid leukaemia and related malignancies (group L3)

Para-meter	EAR_{TLS}		EAR_{QDR}		ERR_{TLS}		ERR_{QDR}	
	MLE	σ	MLE	σ	MLE	σ	MLE	σ
β_1	0.675	0.165	0.678	0.163	0.623	0.164	0.617	0.162
β_2	−0.397	0.161	−0.379	0.156	−0.319	0.157	−0.310	0.152
β_3	3.952	0.761	3.975	0.750	3.584	0.441	3.587	0.441
β_4	3.700	0.713	3.661	0.683	1.633	0.269	1.635	0.269
β_5	1.216	0.749	1.243	0.729	0.135	0.081	0.134	0.079
β_6	1.868	0.463	1.831	0.452	−0.208	0.050	−0.199	0.048
β_7	0.166	0.082	0.166	0.080	−0.313	0.242	−0.328	0.240
β_8	−0.180	0.049	−0.174	0.046	−0.184	0.393	−0.199	0.391
β_9	−0.311	0.243	−0.329	0.240	0.008	0.127	0.017	0.125
β_{10}	−0.183	0.393	−0.201	0.391	0.312	0.073	0.299	0.073
β_{11}	2.556	0.858	2.585	0.843	0.773	0.437	0.741	0.430
β_{12}	1.406	0.477	1.426	0.467	0.748	0.175	0.834	0.340
β_{13}	0.718	0.195	1.587	0.370	0.346	0.249		
β_{14}	0.704	0.456			2.809	1.260		
β_{15}	5.250	1.846						

and the risk functions of EAR-type appear as follows for linear spline dose response:

$$EAR_{TLS}(10^{-4}PY^{-1}) = \exp\left[\beta_{11}\ln\frac{a}{70} + \beta_{12}\ln^2\frac{a}{70}\right] \times$$
$$\times \begin{cases} \beta_{14}D & \text{if } D < \beta_{13} \\ \beta_{13}\beta_{14} + \beta_{15}(D - \beta_{13}) & \text{otherwise} \end{cases} \tag{13.12}$$

and for pure quadratic dose response:

$$EAR_{QDR}(10^{-4}PY^{-1}) = \exp\left[\beta_{11}\ln\frac{a}{70} + \beta_{12}\ln^2\frac{a}{70}\right] \times 1.12D^2\beta_{13}. \tag{13.13}$$

Parameter of the models and their standard deviations are shown in Table 13.3.

As follows from the above equations (13.8)–(13.13), the four selected models form two pairs of 'twins'. Namely, ERR_{TLS} (13.9) and ERR_{QDR} (13.10) make the first pair of the twin models, while EAR_{TLS} (13.12) and EAR_{QDR} (13.13) – the second pair.

13.4 Leukaemia group L4 (CML)

The group L4 (code 204) combines together 73 cases of chronic myeloid leukaemia (CML, ICD10:C92.1), 8 cases 'not-in-city' at the time of bombing.

The fitting resulted in a group of six models, four of ERR-type and two of EAR-type. These models are:

- ERR-t-QE model of ERR-type with quadratic-exponential dose response and time-since-exposure effect modifier ($w_{AIC} = 7.08\%$);

- ERR-t-LNT model of ERR-type with linear dose response and time-since-exposure effect modifier ($w_{AIC} = 21.00\%$);

- ERR-e-QE model of ERR-type with quadratic-exponential dose response and age-at-exposure effect modifier ($w_{AIC} = 1.72\%$);

- ERR-e-LNT model of ERR-type with linear dose response and age-at-exposure effect modifier ($w_{AIC} = 7.00\%$);

- EAR-t-LNT model of EAR-type with linear dose response and time-since-exposure effect modifier ($w_{AIC} = 55.12\%$);

- EAR-e-LNT model of EAR-type with linear dose response and age-at-exposure effect modifier ($w_{AIC} = 8.08\%$).

The four models of ERR-type share the same form of the parametric baseline rate:

$$\lambda_0(10^{-4}PY^{-1}) = \exp\left[\beta_1 + (\beta_2 m + \beta_3 f)\ln\frac{a}{70} + \beta_4 NIC_{Hi} + \beta_5 NIC_{Na}\right]. \tag{13.14}$$

For the ERR-type models, the risk functions appear as follows:

$$ERR_{tQE} = \exp\left[\beta_6 \ln\frac{a}{55} + \frac{\beta_7}{10}\ln\frac{a-e}{25} + \beta_8 n\right] \times 1.12\beta_9 D^2 \exp(\beta_{10}D), \tag{13.15}$$

$$ERR_{tLNT} = \exp\left[\beta_6 \ln\frac{a}{55} + \frac{\beta_7}{10}\ln\frac{a-e}{25} + \beta_8 n\right] \times \beta_9 D \tag{13.16}$$

if time since exposure is selected as an effect modifier for risk, and

$$ERR_{eQE} = \exp\left[\beta_6 \ln\frac{a}{55} + \beta_7 \ln^2\frac{a}{55} + \beta_8\frac{e-30}{10} + \beta_9 n\right] \times 1.12\beta_{10} D^2 \exp(\beta_{11}D), \tag{13.17}$$

$$ERR_{eLNT} = \exp\left[\beta_6 \ln\frac{a}{55} + \beta_7 \ln^2\frac{a}{55} + \beta_8\frac{e-30}{10} + \beta_9 n\right] \times \beta_{10} D \tag{13.18}$$

if age at exposure is used to modify radiation risk.

The two models of EAR-type also have their common, sex-independent, structure of simple parametric baseline:

$$\lambda_0(10^{-4}PY^{-1}) = \exp\left[\beta_1 + \beta_2 \ln\frac{a}{70} + \beta_3 NIC_{Hi} + \beta_4 NIC_{Na}\right]. \tag{13.19}$$

Radiation-attributed excess rates for the EAR-type models appear as follows:

$$EAR_{tLNT}(10^{-4}PY^{-1}) = \exp\left[\beta_5 f \ln\frac{a}{55} + \frac{\beta_6}{10}\ln\frac{a-e}{25}\right] \times \beta_7 D, \qquad (13.20)$$

$$EAR_{eLNT}(10^{-4}PY^{-1}) = \exp\left[(\beta_5 m + \beta_6 f)\ln\frac{a}{55} + \beta_7 \ln^2\frac{a}{55} + \beta_8\frac{e-30}{10}\right] \times \beta_9 D. \qquad (13.21)$$

Of the six model belonging to the group L4, the four models of ERR-type are treated as twin models. That is, the higher risk values obtained from the pair of models ERR_{tQE} (13.15) and ERR_{tLNT} (13.16) or from the another pair, ERR_{eQE} (13.17) and ERR_{eLNT}, (13.18) are used for calculation of assigned share.

Table 13.4: Maximum likelihood estimates and standard deviations of the model parameters selected to describe radiation risk of chronic myeloid leukaemia (group L4)

Parameter	EAR_{tLNT}		EAR_{eLNT}		ERR_{tLNT}		ERR_{tQE}		ERR_{eLNT}		ERR_{eQE}	
	MLE	σ	MLE	σ	MLE	σ	MLE	σ	MLE	σ	MLE	σ
β_1	−1.551	0.210	−1.535	0.210	−1.554	0.207	−1.472	0.193	−1.555	0.208	−1.474	0.194
β_2	2.284	0.662	2.358	0.671	1.322	0.615	1.200	0.546	1.361	0.627	1.212	0.545
β_3	−0.162	0.427	−0.169	0.426	3.149	0.679	3.023	0.636	3.189	0.702	3.036	0.645
β_4	−0.807	1.020	−0.811	1.020	−0.188	0.425	−0.286	0.418	−0.182	0.425	−0.282	0.418
β_5	2.187	0.932	−5.658	1.588	−0.835	1.019	−0.939	1.016	−0.827	1.019	−0.935	1.016
β_6	−16.650	3.330	−3.257	1.597	−1.374	0.731	−1.336	0.671	−6.545	1.647	−6.648	1.662
β_7	0.599	0.203	−1.762	0.794	−15.951	3.443	−16.678	3.668	−1.551	0.746	−1.570	0.759
β_8			1.005	0.262	−1.499	0.744	−1.710	0.757	0.966	0.255	1.006	0.274
β_9			0.608	0.239	5.275	2.333	10.533	6.311	−1.489	0.741	−1.707	0.756
β_{10}									5.643	2.700	11.347	7.125
β_{11}							−0.752	0.289			−0.761	0.288

Acknowledgements

Bibliography

BEIR (1999). *Health effects of exposure to radon.* Committee on Health Risks of Exposure to Radon (BEIR VI). Board on Radiation Effects Research, Commission on Life Sciences, National Research Council. National Academy Press.

BEIR (2006). *Health Risks from Exposure to Low Levels of Ionizing Radiation: BEIR VII Phase 2.* National Academies Press.

Brenner, A. V., Tronko, M. D., Hatch, M., Bogdanova, T. I., Oliynik, V. A., Lubin, J. H., Zablotska, L. B., Tereschenko, V. P., McConnell, R. J., Zamotaeva, G. A., O'Kane, P., Bouville, A. C., Chaykovskaya, L. V., Greenebaum, E., Paster, I. P., Shpak, V. M., and Ron, E. (2011). I-131 dose response for incident thyroid cancers in Ukraine related to the Chornobyl accident. *Environmental Health Perspectives*, 119(7):933–939.

Cardis, E., Kesminiene, A., Ivanov, V., Malakhova, I., Shibata, Y., Khrouch, V., Drozdovitch, V., Maceika, E., Zvonova, I., Vlassov, O., Bouville, A., Goulko, G., Hoshi, M., Abrosimov, A., Anoshko, J., Astakhova, L., Chekin, S., Demidchik, E., Galanti, R., Ito, M., Korobova, E., Lushnikov, E., Maksioutov, M., Masyakin, V., Nerovnia, A., Parshin, V., Parshkov, E., Piliptsevich, N., Pinchera, A., Polyakov, S., Shabeka, N., Suonio, E., Tenet, V., Tsyb, A., Yamashita, S., and Williams, D. (2005). Risk of thyroid cancer after exposure to 131I in childhood. *Journal of the National Cancer Institute*, 97(10):724–732.

Chmelevsky, D., Nekolla, E., and Barclay, D. (1995). *Strahlenepidemiologische Tabellen: die Berechnung von Verursachungswahrscheinlichkeiten bösartiger Neubildungen nach vorausgegangener Strahlenexposition.* Schriftenreihe Reaktorsicherheit und Strahlenschutz. grm, Merkel.

Darby, S., Hill, D., Auvinen, A., Barros-Dios, J. M., Baysson, H., Bochicchio, F., Deo, H., Falk, R., Forastiere, F., Hakama, M., Heid, I., Kreienbrock, L., Kreuzer, M., Lagarde, F., Mäkeläinen, I., Muirhead, C., Oberaigner, W., Pershagen, G., Ruano-Ravina, A., Ruosteenoja, E., Rosario, A. S., Tirmarche, M., Tomásek, L., Whitley, E., Wichmann, H.-E., and Doll, R. (2005). Radon in homes and risk of lung cancer: collaborative analysis of individual data from 13 European case-control studies. *BMJ (Clinical research ed.)*, 330(7485):223.

Darby, S., Hill, D., Deo, H., Auvinen, A., Barros-Dios, J. M., Baysson, H., Bochicchio, F., Falk, R., Farchi, S., Figueiras, A., Hakama, M., Heid, I., Hunter, N., Kreienbrock, L., Kreuzer, M., Lagarde, F., Mäkeläinen, I., Muirhead, C., Oberaigner, W., Pershagen, G., Ruosteenoja, E., Rosario, A. S., Tirmarche, M., Tomásek, L., Whitley, E., Wichmann, H.-E., and Doll, R. (2006). Residential radon and lung cancer–detailed results of a collaborative analysis of individual data on 7148 persons with

lung cancer and 14,208 persons without lung cancer from 13 epidemiologic studies in Europe. *Scandinavian Journal of Work, Environment & Health*, 32 Suppl 1:1–83.

Fenske, N. (2015). Parameters of the BfS model for radiation risk of lung cancer due to radon exposure in Wismut cohort after 1960. Personal communication.

Forman, D., Bray, F., Brewster, D., Gombe Mbalawa, C., Kohler, B., Piñeros, M., Steliarova-Foucher, E., Swaminathan, R., and Ferlay, J., editors (2014). *Cancer Incidence in Five Continents, Vol. X. IARC Scientific Publication No. 164.* Lyon: International Agency for Research on Cancer.

Furukawa, K., Preston, D., Funamoto, S., Yonehara, S., Ito, M., Tokuoka, S., Sugiyama, H., Soda, M., Osaza, K., and Mabuchi, K. (2013). Long-term trend of thyroid cancer risk among Japanese atomic-bomb survivors: 60 years after exposure. *Int J Cancer*, 132(5):1222–1226.

Furukawa, K., Preston, D. L., Löhn, S., Funamoto, S., Yonehara, S., Matsuo, T., Egawa, H., Tokuoka, S., Ozasa, K., Kasagi, F., Kodama, K., and Mabuchi, K. (2010). Radiation and smoking effects on lung cancer incidence among atomic bomb survivors. *Radiation Research*, 174:72–82.

Hayashi, Y., Lagarde, F., Tsuda, N., Funamoto, S., Preston, D., Koyama, K., Mabuchi, K., Ron, E., Kodama, K., and Tokuoka, S. (2010). Papillary Microcarcinoma of the Thyroid among Atomic Bomb Survivors: Tumor Characteristics and Radiation Risk. *Cancer*, 116(7):1646–1655.

Hsu, W.-L., Preston, D. L., Soda, M., Sugiyama, H., Funamoto, S., Kodama, K., Kimura, A., Kamada, N., Dohy, H., Tomonaga, M., et al. (2013). The incidence of leukemia, lymphoma and multiple myeloma among atomic bomb survivors: 1950-2001. *Radiation Research*, 179(3):361–382.

ICRP (1993). Radon-222 at Home and at Work ICRP Publication 65. *ICRP Publication*, 65.

ICRP (2007). The 2007 Recommendations of the International Commission on Radiological Protection. ICRP Publication 103. *Ann. ICRP*, 37(2-4).

ICRP (2010). Lung Cancer Risk from Radon and Progeny and Statement on Radon. ICRP Publication 115. *Annals of the ICRP*, 40(1):1–64.

ICRP (2014). Radiological Protection against Radon Exposure. ICRP Publication 126. *Annals of the ICRP*, 43(3):5–73.

ICRP (2015). Occupational Intakes of Radionuclides: Part 1. *Annals of the ICRP*, 44(2).

Jacob, P., Bogdanova, T., Buglova, E., Chepurniy, M., Demidchik, Y., Gavrilin, Y., Kenigsberg, J., Meckbach, R., Schotola, C., Shinkarev, S., Tronko, M., Ulanovsky, A., Vavilov, S., and Walsh, L. (2006). Thyroid cancer risk in areas of Ukraine and Belarus affected by the Chernobyl accident. *Radiation Research*, 165:1–8.

Jacob, P., Kaiser, J., and Ulanovsky, A. (2013). ProZES – a tool for assessment of assigned share of radiation in probability of cancer development. Research report, Institute of Radiation Protection, Helmholtz Zentrum München—German Research Center for Environmental Health, Neuherberg.

Jacob, P., Kaiser, J., and Ulanovsky, A. (2014a). Ultrasonography survey and thyroid cancer in the Fukushima Prefecture. *Radiat Environ Biophys*, 53:391–401.

Jacob, P., Kaiser, J. C., and Ulanovsky, A. (2014b). Erratum to: Ultrasonography survey and thyroid cancer in the Fukushima Prefecture. *Radiat Environ Biophys*, 53:403.

Kaiser, J. and Walsh, L. (2015). Analysis and descriptive modelling of the LSS skin cancer data. Personal communication.

Kocher, D., Apostoaei, A., Hoffman, F., Schubauer-Berigan, M., Stancescu, D., Thomas, B., Trabalka, J., Gilbert, E., and Land, C. (2008). Interactive radioepidemiological program (IREP): a web-based tool for estimating probability of causation/assigned share of radiogenic cancers. *Health Physics*, 95(1):119–147.

Konno, R., Sagae, S., Yoshikawa, H., Basu, P. S., Hanley, S. J. B., Tan, J. H. J., and Shin, H.-R. (2010). Cervical Cancer Working Group report. *Japanese Journal of Clinical Oncology*, 40 Suppl 1:i44–i50.

Kopecky, K. J., Stepanenko, V., Rivkind, N., Voillequé, P., Onstad, L., Shakhtarin, V., Parshkov, E., Kulikov, S., Lushnikov, E., Abrosimov, A., Troshin, V., Romanova, G., Doroschenko, V., Proshin, A., Tsyb, A., and Davis, S. (2006). Childhood thyroid cancer, radiation dose from Chernobyl, and dose uncertainties in Bryansk Oblast, Russia: a population-based case-control study. *Radiation Research*, 166(2):367–374.

Kraemer, A., Chen, I.-P., Henning, S., Faust, A., Volkmer, B., Atkinson, M. J., Moertl, S., and Greinert, R. (2013). UVA and UVB irradiation differentially regulate microRNA expression in human primary keratinocytes. *PLoS ONE*, 8(12):e83392.

Kreuzer, M., Fenske, N., Schnelzer, M., and Walsh, L. (2015). Lung cancer risk at low radon exposure rates in German uranium miners. *British Journal of Cancer*, 113(9):1367–1369.

Land, C., Gilbert, E., Smith, J., Hoffman, F., Apostoaei, I., Thomas, B., and Kocher, D. (2003). *Report of NCI-CDC Working Group to revise the 1985 NIH radioepidemiological tables.*, volume 03-5387. National Institutes of Health, National Cancer Institute, NIH Publication.

Leuraud, K., Schnelzer, M., Tomasek, L., Hunter, N., Tirmarche, M., Grosche, B., Kreuzer, M., and Laurier, D. (2011). Radon, Smoking and Lung Cancer Risk: Results of a Joint Analysis of Three European Case-Control Studies Among Uranium Miners. *Radiation Research*, 176:375–387.

MathWorks (2015). *Optimization Toolbox. User's Guide.* The MathWorks, Inc., Natick, MA.

NCC (2013). *National estimates of cancer incidence based on cancer registries in Japan (1975-2010).* Cancer Information Service, National Cancer Center, Japan.

Niu, S., Deboodt, P., and Zeeb, H., editors (2010). *Approaches to attribution of detrimental health effects to occupational ionizing radiation exposure and their application in compensation programmes for cancer: A practical guide.*, volume 73 of *Occupational Safety and Health Series.* International Atomic Energy Agency, the International Labour Organization and the World Health Organization.

Preston, D. (2011). Numerical values of the parameters of the lung cancer models. Personal communication.

Preston, D., Ron, E., Tokuoka, S., Funamoto, S., Nishi, N., Soda, M., Mabuchi, K., and Kodama, K. (2007). Solid cancer incidence in atomic bomb survivors: 1958–1998. *Radiation Research*, 168:1–64.

Preston, D. L., Lubin, J. H., Pierce, D. A., McConney, M. E., and Shilnikova, N. S. (2015). *EPICURE Version 2. User Guide.* Risk Sciences International.

RKI (2013). *Krebs in Deutschland 2009/2010. 9. Ausgabe. Beiträge zur Gesundheitsberichterstattung des Bundes.* . Robert Koch-Institut und die Gesellschaft der epidemiologischen Krebsregister in Deutschland e.V.

Takatsuki, K. (2005). Discovery of adult T-cell leukemia. *Retrovirology*, 2(1):16.

Tronko, M. D., Brenner, A. V., Olijnyk, V. A., Robbins, J., Epstein, O. V., McConnell, R. J., Bogdanova, T. I., Fink, D. J., Likhtarev, I. A., Lubin, J. H., Markov, V. V., Bouville, A. C., Terekhova, G. M., Zablotska, L. B., Shpak, V. M., Brill, A. B., Tereshchenko, V. P., Masnyk, I. J., Ron, E., Hatch, M., and Howe, G. R. (2006). Autoimmune thyroiditis and exposure to iodine 131 in the Ukrainian cohort study of thyroid cancer and other thyroid diseases after the Chornobyl accident: results from the first screening cycle (1998-2000). *The Journal of clinical endocrinology and metabolism*, 91(11):4344–4351.

Tsuji, I. (2009). Current Status of and Future Outlook for Cancer Screening in Japan. *Breast cancer*, 400(300):200.

UNSCEAR (2009). *Effects of Ionizing Radiation: UNSCEAR 2006 Report to the General Assembly, with Scientific Annexes. Annex E Sources-to-effects assessment for radon in homes and workplaces.* Number v. 2 in Effects of Ionizing Radiation: UNSCEAR 2006 Report to the General Assembly, with Scientific Annexes. UN.

UNSCEAR (2011). *Summary of low-dose radiation effects on health. United Nations Scientific Committee on the Effects of Atomic Radiation (UNSCEAR) 2010 Report to the General Assembly.* United Nations.

Walsh, L., Grosche, B., Schnelzer, M., Tschense, A., Sogl, M., and Kreuzer, M. (2015). A review of the results from the German Wismut uranium miners cohort. *Radiation Protection Dosimetry*, 164(1-2):147–153.

Young, R. and Kerr, G., editors (2005). *Reassessment of the atomic bomb radiation dosimetry for Hiroshima and Nagasaki: Dosimetry System 2002.* Radiation Effects Research Foundation.

| Verantwortung für Mensch und Umwelt |

Bundesamt für Strahlenschutz